WADC TECHNICAL REPORT 55-226

EFFECT OF CYCLIC LOAD FREQUENCY ON THE CREEP-RUPTURE AND FATIGUE PROPERTIES OF JET ENGINE MATERIALS

L. A. YERKOVICH

G. J. GUARNIERI

CORNELL AERONAUTICAL LABORATORY, INC.

DECEMBER 1955

MATERIALS LABORATORY
CONTRACT No. AF 33(616)-42
PROJECT No. 7360
TASK No. 73604

WRIGHT AIR DEVELOPMENT CENTER
AIR RESEARCH AND DEVELOPMENT COMMAND
UNITED STATES AIR FORCE
WRIGHT-PATTERSON AIR FORCE BASE, OHIO

Carpenter Litho & Prtg. Co., Springfield, O.
300 - April 1956

FOREWORD

This report was prepared by Cornell Aeronautical Laboratory, Inc. under USAF Contract No. AF 33(616)-42 and covers work during the period of March 1952 to February 1955. The contract was initiated under Project No. 7360 "Materials Analysis and Evaluation Techniques", Task No. 73604 "Fatigue Properties of Structural Materials", formerly RDO No. 614-16, and was administered under the direction of the Materials Laboratory, Directorate of Research, Wright Air Development Center, with Lt. C. L. Harmsworth acting as project engineer.

ABSTRACT

An investigation has been conducted to evaluate the effects of cyclic loading and load frequency on the elevated temperature creep rupture properties of several jet engine sheet materials. Specifically the behaviors of low carbon N-155, type 321 stainless steel and Inconel X were studied, when exposed to various combined steady and cyclic stresses at various stress amplitudes and temperatures within a wide range of test frequencies.

Data for selected static and dynamic test conditions are presented in various tabular and chart forms to illustrate the influence of direct fluctuating stresses on the creep and rupture characteristics of the test alloys. These data demonstrate that the static load high temperature creep and rupture behavior of N-155, type 321 stainless steel and Inconel X are not always altered by the superposition of cyclic stresses; however, damage may be accelerated or retarded depending upon temperature, static stress level and the frequency of the cyclic stress component.

PUBLICATION REVIEW

This report has been reviewed and is approved.

FOR THE COMMANDER:

M. R. WHITMORE
Technical Director
Materials Laboratory
Directorate of Research

TABLE OF CONTENTS

LIST OF TABLES

LIST OF ILLUSTRATIONS

INTRODUCTION

In recent years, the elevated-temperature properties of alloys suitable for jet-engine applications have been the subject of rather intensive study. While most laboratory investigations have been concerned with defining the creep behavior of alloys under the influence of constant loads and constant temperatures, some information is available regarding the effects on creep generated by temperature and stress fluctuations which simulate conditions encountered in service. Results of creep deformation and rupture determinations under cyclic or intermittent temperatures and stresses were presented in a symposium at the Fifty-Seventh Annual meeting of the American Society for Testing Materials (1)* to illustrate how constant stress and constant temperature behaviors of metals are modified by essentially slow square wave type cycles.

In addition to the intermittent-type simulated-service tests, attention has been directed toward the high-temperature behavior of metals when dynamic sinusoidal type stresses, such as those generated by vibrations, are present. A preliminary investigation of the influence of superimposing a fluctuating stress about a mean stress on creep deformation was made at Cornell Aeronautical Laboratory, Inc. in 1948 which showed the important relationship of creep rate with temperature and frequency of stress fluctuation. Discussion of this investigation was presented at a Project SQUID Conference (2). Lazan (3) and Manjoine (4) at the 1949 annual meeting of the American Society for Testing Materials demonstrated that materials subjected to cyclic stresses about fixed mean stresses at 3600 and 1200 cycles per minute, exhibited deformation effects different from those under static conditions. Gillig and Guarnieri (5) working with Armco iron at 800 and 1000°F have shown that the superposition of a cyclic load upon a static tensile load in a long-time creep test will not necessarily cause deformation to proceed at an increased rate, indicating that the cyclic load characteristics are important in governing deformation behaviors of materials.

The lack of appropriate data, dealing with the high-temperature behavior of materials exposed to stress fluctuations, has imposed a handicap on the design engineer from the standpoint of assigning limiting-stress values to heated members subjected to cyclic tensile stresses in jet-engine service. The design criteria for high-temperature alloys, subjected to stress fluctuations, have been for the most part based on laboratory test performances of these alloys under the separate effects of static creep and fatigue with major consideration given to that property which appears to be more seriously affected under the operating conditions. Actually, the operation of jet propelled aircraft is such as to include the combined effects of creep and fatigue. The extent to which these phenomena are active

*See bibliography.

in a single member exposed to dynamic loads and their relative influences in promoting failure will, of course, depend on a combination of factors of which temperature, mean stress, and frequency and amplitude of the fluctuating stress are most important.

For materials subjected to direct tensile stressing, it has been the intent of this program to establish the influence of the cyclic stress variables, specifically frequency of stressing, as related to temperature and mean stress in promoting damage and to provide representative dynamic stressing data which may be applicable for similar conditions of service loading. Preliminary to this determination, however, attention was devoted to devising cyclic-load creep testing techniques with particular emphasis on the development of methods and equipment capable of providing a variety of sinusoidal direct stress amplitude and frequency patterns which can be controlled and maintained for relatively long periods of time.

TEST MATERIALS AND PROGRAM

Three alloys, all in sheet form, low carbon N-155, Inconel X and type 321 stainless steel, were selected for this investigation because of their high-temperature applications as jet-engine materials. The certified chemical analyses of these alloys, furnished by the Haynes Stellite Company, International Nickel Company, Inc. and American Rolling Mill Company respectively, are illustrated in Table 1 below.

TABLE 1

CHEMICAL COMPOSITIONS OF TEST ALLOYS

	N-155	Inconel X	321 Stainless Steel
C	0.13	0.04	0.07
Si	0.56	0.30	0.50
Mn	1.45	0.71	1.56
S	0.009	0.007	0.012
P	0.023	-	0.023
Fe	Bal.	6.83	Bal.
Ni	19.26	72.63	9.47
Cr	21.01	14.86	17.88
Co	20.17	-	-
Mo	3.16	-	-
W	2.41	-	-
Al	-	1.00	-
Cu	-	0.09	-
Ti	-	2.42	0.66
Ta + Cb	0.86	1.09	-

Low carbon N-155 sheet of 0.044-inch thickness was tested in the "as-received" condition; final mill processing before shipment consisting of an anneal at 2150°F for ten minutes, followed by air cooling.

Inconel X sheet of 0.044-inch thickness was tested after aging at 1550°F for 24 hours, air cooling and subsequently aging at 1300°F for 20 hours, followed by air cooling.

Type 321 stainless steel sheet of 0.049-inch thickness was tested in the "as-received" condition mill processed, before shipment, to a 2D finish.

The room temperature strength properties of these alloys as determined for the longitudinal direction are presented in Table 2, as follows:

TABLE 2

ROOM TEMPERATURE MECHANICAL PROPERTIES OF TEST ALLOYS

Alloy	Rockwell Hardness	0.2% Yield Strength PSI	Ultimate Tensile Strength PSI	% Elongation in 2 Inches
Low Carbon N-155	RB 90	58,200	118,500	56.0
	RB 89	57,800	120,800	56.0
Inconel X	RC 31	100,500	168,500	22.5
	RC 30		168,300	23.5
Type 321 Stainless Steel	RB 74	38,200	87,800	54.0
	RB 75	35,300	89,200	63.0

All test alloys were investigated at 1500°F with additional testing on low carbon N-155 and Inconel X at 1350°F. Conditions of sinusoidal direct tensile stressing were used to compare the effects of frequency and amplitude of superimposed tensile stresses on their high-temperature creep and rupture properties with those obtained by static loading. In the test program, fluctuating tensile stresses equal to ± 0, 25, and 67% of selected static stresses were superimposed upon the various static stresses at frequencies of 0, 11.5, 115, 3600, and 14,400 cycles per minute to represent a rather wide range of the frequency variable.

TEST EQUIPMENT AND PROCEDURE

Static Test Procedure

The initial portion of this investigation concerned with the determination of reference data has been performed with the use of the conventional lever-type creep apparatus. Test temperature is maintained with a resistance wound creep furnace provided with appropriate shunts to adjust temperature distribution in the top, middle, or bottom furnace sections as required and regulated to provide low or high voltage input to the furnace by a conventional potentiometric temperature controller. With this system of control and adjustment, the test temperature is maintained within limits of ± 3°F of the nominal test temperature over a two-inch gage section for the duration of the test. Temperature measurements are made at the top, middle, and bottom gage section by calibrated chromel-alumel thermocouples wired to the specimen at those positions and shielded from furnace radiation by asbestos cord. A precision

potentiometer, accurate to within one-half of 1°F is used to indicate the test section temperature and to serve as a guide for temperature adjustment.

Specimen strain is measured by a set of extensometers attached to a two-inch specimen gage section. These extensometers engage cantilever beams to which resistance strain gages are cemented. The displacement of the extensometers, being a direct measure of the creep deformation, is transmitted to the cantilever pickup system and is detected as an unbalance in an electrical bridge circuit. Precalibration of the beams and the bridge circuit permits convenient and accurate conversion of the generated bridge unbalance into creep strain. Continuous record of the strain is made on a Dynalog type strain recorder with a long time accuracy of 0.0003 inch and a sensitivity of 0.00003 inch per inch. The method of strain measurement is illustrated in Figure 1 which shows the essential features in the specimen-extensometer-thermocouple assembly.

Low-Frequency Cyclic-Load Test Procedure

The test equipment to carry out the low frequency cyclic-loading portion of the investigation consists basically of the conventional lever type static-creep test apparatus to which have been added facilities for the superposition of fluctuating stresses on the test specimen. Temperature control and deformation measurement techniques identical to those described for the static test procedure were employed.

Since the low frequency tests (11.5 and 115 cpm) are within the range where inertia effects of moving components are of minor significance, standard lever type creep units were modified to allow superimposed cyclic loads to be applied to the lever through a spring driven by an eccentric at the appropriate frequency. In the case where creep deformation occurs, some provision must be made to maintain the spring deflection constant as the loading beam is displaced. To accomplish this compensation for creep, a take-up motor which becomes energized through the movement of the beam has been installed in the loading circuit to control spring deflection.

Accurate measurement of the dynamic load is made with SR-4 resistance strain gages cemented to a room temperature link below and in series with the test specimen. With the use of appropriate strain-analyzing instrumentation and static-load calibrations prior to the start of each test, the stress pattern in the specimen is determined and adjusted. The essential features of the test apparatus are illustrated schematically in Figure 2 to show the method of stress cycling and the various control and stress measuring instrumentation employed.

High-Frequency Cyclic-Load Test Procedure

In conducting the high-frequency cyclic test program, equipment was designed incorporating the temperature control and strain measuring features described in the static test procedure. For this series of tests which required relatively large loads to be cycled at 3,600 and 14,400 cycles per minute, test units were constructed employing electromagnetic vibrators as the cyclic stress source.

As in the low-frequency test program, stress adjustment and measurement are determined by a room-temperature strain link placed in series with the specimen. By a direct static calibration, prior to commencing a test, changes in gage resistance are measured by a strain analyzer and the desired mean load is then applied to the specimen through a caged helical compression spring. Dynamic loads also determined by the strain link, are supplied by the electromagnetic vibrators connected by flexure rods to the specimen and spring assembly. By adjusting the amount of mass in series with the test specimens, cyclic load applications can be regulated to produce the superposition of large amplitude sinusoidal stresses in the neighborhood of the resonant frequency of the mechanical system.

Because creep deformation of the specimen will affect the static load component imposed on a specimen by the spring dynamometer, an automatic creep compensator is required in the loading system. The strain link, in addition to serving its purpose for determining the mean and dynamic stresses applied to the specimen, is used, in conjunction with a combined strain recorder-controller, to energize the creep compensator for maintaining a desired mean stress condition throughout any test. Figure 3 presents schematically the various equipment and instrument relationships in conducting these high frequency dynamic creep tests (6).

TEST RESULTS

Low Carbon N-155

To demonstrate the influence of cyclic stress components on the creep and rupture behavior of low carbon N-155, data illustrating its static (constant load-constant temperature) behavior were determined to provide a necessary reference for comparison. These static base line data are summarized in Table 6 for various selected stresses at both the 1350 and 1500°F temperature levels.

The creep and rupture characteristics of N-155 under conditions of positive sinusoidal cyclic stressing through the frequency range of 11.5 to 14,400 cycles per minute and cyclic stress amplitudes of ± 25 and 67% at 1350 and 1500°F are presented in Tables 7 through 10. Graphic representation of the 1350°F data showing the relationship of mean stress and time, as affected by stressing frequency and compared with static behavior for selected deformation levels and rupture, are illustrated in Figures 4 and 5 for the ± 25 and 67% cyclic stress amplitudes respectively. Similar mean stress-time relationships comparing the 1500°F static and ± 25 and 67% cyclic stress amplitude characteristics are presented in Figures 6 and 7 respectively.

Inasmuch as stress amplitude constitutes another important variable controlling the cyclic-load, high-temperature deformation and rupture properties of materials, the effects of amplitude can be shown by replotting the test data at constant frequencies and constant temperatures. For the range of cyclic-stress amplitudes from 0 (static) to ± 67% of mean load, curves relating mean tensile stress and alternating tensile stress are graphically illustrated in Figure 8 at 1350 and in Figure 9 at 1500°F. Presented in this form, the data not only illustrate the influence of cyclic stress amplitudes on the creep and rupture characteristics of low carbon N-155, but also provide a very convenient guide for selecting limiting steady and cyclic stress combinations.

The over-all effect of stress cycling on the rupture characteristics of low carbon N-155 can be demonstrated by establishing a ratio of cyclic mean-rupture stress to static-rupture stress for specific rupture times up to 500 hours. This ratio when less than one signifies that the cyclic stress component induces a damaging effect in excess of the static mean stress on the test alloy and when greater than one indicates that damage is retarded by cyclic stressing. For the time range under consideration and the particular combinations of temperature and cyclic stress, these ratios are summarized in Table 3, page 8.

TABLE 3

MEAN STRESS RATIOS TO PRODUCE RUPTURE OF N-155 ALLOY UNDER CYCLIC LOAD AS COMPARED TO STATIC LOAD

Temp. °F	Cyclic Stress Amplitude %	Cyclic Stress Frequency CPM	Ratio Cyclic Mean Rupture Stress to Static Rupture Stress 10 Hours	20 Hours	50 Hours	100 Hours	200 Hours	500 Hours
1350	± 25	115	0.99	1.00	1.00	0.96	0.94	0.92*
		3,600	1.00	0.97	0.97	0.97	0.97	1.02*
		14,400	0.86	0.83	0.82	0.83	0.80	0.82
	± 67	115	0.70	0.69	0.71	0.75	0.77	0.81
		3,600	0.85*	0.81*	0.82	0.88	0.90	0.95*
1500	± 25	11.5	0.98*	0.95*	0.94	0.93	0.93	0.94
		115	1.03	1.00	1.03	1.05	1.04	0.99
		3,600	1.04	1.02	1.03	1.01	1.03	1.01
		14,400	0.90*	0.87	0.89	0.92	0.87	0.79
	± 67	115	0.87	0.85	0.88	0.90	0.90	0.88
		3,600	0.85	0.86	0.93	0.92	0.86	0.79

*Ratio calculated from extrapolated stress values.

From the above tabulation of ratios, the variables of temperature, cyclic stress, amplitude and cyclic stressing frequency can very appropriately be analyzed according to their respective influences on the rupture characteristics of the test alloy. It can be seen, for example, at both the 1350 and 1500°F temperature levels, that for constant stress amplitudes of ± 25% cycled at 11.5, 115, and 3600 cycles per minute, there appears to be no significant change in the mean stress to rupture values throughout the time range in that the ratios fall within the range of reproducibility in creep-rupture testing. When stressing frequency at the constant ± 25% amplitude is increased to 14,400, the test alloy N-155 displays an appreciable decrease in cyclic mean stress to produce rupture in the equivalent time, and this decrease appears to become more pronounced with increasing time to rupture. Likewise, at fixed frequencies for both temperatures, increasing cyclic stress amplitude from ± 25 to ± 67% results in a substantial decrease at a definite time level to rupture of the cyclic mean stress which tends to diminish with increasing rupture time at 1350 and remains relatively uniform at 1500°F. It is further observed that the ± 67% cyclic component at 1350°F is more damaging when applied at 115 cpm than at 3600 cpm and more damaging than the 1500°F ± 67% cyclic component applied at the same 115 cpm test frequency.

Because alloys generally exhibit varying degrees of sensitivity to stress in their creep-deformation and rupture behavior with temperature changes, it might be expected that as temperature is varied, the effect of cyclic stressing will be to alter the mode of damage from a time-dependent to a cyclic-dependent type or vise versa. In this event, an analysis of the test results from a standpoint of failure according to the number of stress cycle applications appears to be appropriate. These data summarizing the stress and cycle dependent characteristics at both 1350 and 1500°F are presented in Table 11 and are graphically represented in Figure 10 as typical S-N curves relating the number of cycles to failure with the maximum stress developed in the stress cycle. Examination of the curves over the frequency range up to 3600 cycles per minute indicates that at both the 1350 and 1500°F temperature levels rupture is predominantly time-dependent. In the frequency range between 3600 and 14,400 cycles per minute there is a trend toward cyclic-dependency which is suggested by the near matching of the ± 25% amplitude lines at these frequencies. Along with these observations it might appear off hand, due to the almost consistent upward displacement of the ± 67% amplitude lines over the corresponding ± 25% amplitude lines, that improvement is induced by increasing stress amplitude. It must be pointed out, however, that for the same maximum stress levels, mean stress for the ± 67% amplitude condition must necessarily be less than that of the ± 25% amplitude condition, thus creating a less severe creep condition for the 67% amplitude tests than for the 25% amplitude ones at the same maximum stress level.

Inconel X

Like low carbon N-155, Inconel X was also subjected to cyclic stress conditions in the 1350 to 1500°F temperature range. Prior to conducting the cyclic stress program on this alloy, the static stress base line creep-rupture data were determined at the 1350 and 1500°F temperature levels to provide the reference by which cyclic stressing effects could be evaluated. These reference creep-rupture data are summarized in Table 12 for the various selected static stresses applied.

The cyclic creep and rupture behaviors of Inconel X, for the ± 25 and 67% cyclic stress amplitude series applied at frequencies of 115, 3600, and 14,400 cycles per minute and temperatures of 1350 and 1500°F, are presented in Tables 13 through 15. These data are graphically illustrated in the conventional mean stress-time charts, along with the appropriate static results, for several amounts of total deformation and rupture at constant cyclic stress amplitude and constant temperature in Figures 11 through 14 to demonstrate the influence of the frequency factor on the high-temperature deformation and rupture characteristics of Inconel X. In addition, the relationship of mean stress and alternating stress

for the static and cyclic conditions of testing are presented in Figures 15 and 16 to illustrate the manner in which cyclic stress amplitude affects the static behavior of this alloy at the selected frequencies.

Again, by expressing the time-dependent rupture characteristics of Inconel X in terms of cyclic mean rupture stress to static rupture-stress ratios, the variables of temperature, stress amplitude, and stressing frequency can be analyzed either as to their individual or combined influences in promoting rupture throughout a definite time range. These mean rupture-stress ratios are summarized in Table 4 as follows:

TABLE 4

MEAN STRESS RATIOS TO PRODUCE RUPTURE OF INCONEL X UNDER CYCLIC LOAD AS COMPARED TO STATIC LOAD

Temp. °F	Cyclic Stress Amplitude %	Cyclic Stress Frequency CPM	Ratio Cyclic Mean Rupture Stress to Static Rupture Stress 10 Hours	20 Hours	50 Hours	100 Hours	200 Hours
1350	± 25	115	0.95	0.93	0.95	0.96	1.00
		3,600	1.00	0.94	0.94	0.94	0.98
		14,400				1.23	1.03
	± 67	115	0.74	0.73	0.77	0.81	0.87
		3,600				1.19*	0.94
1500	± 25	115	1.00	0.97	0.97	0.98	1.04*
		3,600	1.00	0.95	0.92	0.98	1.06*
		14,400	0.80*	0.78	0.83	0.94	0.99
	± 67	115	0.75	0.76	0.78	0.83	0.91
		3,600	0.90	0.88	0.89	0.88	0.95

*Ratio calculated from extrapolated stress values.

At both temperatures the stress ratios indicate that the ± 25% cyclic stress component imparts little or no effect on static rupture stress at stressing frequencies of 115 and 3600 cycles per minute. However, at 1500°F when the ± 25% cyclic stress amplitude is applied at 14,400 cycles per minute a substantial loss in rupture strength occurs although the effect diminishes with increased rupture time. For the ± 67% stress amplitude series at 1500°F, the fluctuating stress component has the effect of promoting damage at both the 115 and 3600 cpm frequencies; however, at the 115 cpm frequency, damage is reduced with time while at 3600 cpm it appears

to be somewhat uniform and independent of time.

The 1350°F characteristics of Inconel X under a ± 25% stress amplitude cycled at 14,400 cycles per minute and ± 67% stress amplitude at 3600 cycles per minute are particularly significant in that the ratios show improvement in rupture behavior associated with cyclic stressing with the effect diminishing with test time. This behavior for Inconel X does not follow the usual trends with regard to mean rupture stress and time exhibited for the other conditions of cyclic stressing and may imply that at 1350°F for these very high strain rates, the alloy is displaying a sensitivity to the number of stress cycle applications.

To illustrate the response of the test alloy to stress cycles or more specifically to the number of stress cycles, the test data have been compiled in Table 16 which permits an analysis of the rupture characteristics on a cyclic-dependent basis. The typical S-N curves relating the maximum stress developed in the cycle with cycles to failure for all conditions of test frequency, stress amplitude, and temperature are summarized in Figure 17. It is apparent from the large spread in the 115 and 3600 cpm frequency lines at 1500°F that rupture is essentially time dependent. However, at the high rates of straining generated by stressing at the 14,400 cpm frequency at 1500 and 1350°F and the superposition of the ± 67% cyclic component at 3600 cpm and 1350°F, the combinations of time and number of applied cycles seem to become more significant in promoting rupture.

Type 321 Stainless Steel

In addition to the previous test alloys, type 321 stainless steel was exposed to various cyclic and steady stress conditions to observe its behavior with regard to frequency and amplitude of stressing at 1500°F. The base line data indicating the static creep and rupture characteristics of this alloy are summarized in Table 17. Cyclic data determined at 1500°F for the ± 25 and 67% stress amplitude series applied at test frequencies of 11.5, 115, 3600, and 14,400 cycles per minute are presented in Tables 18 through 21. Graphical representations of the cyclic stressing characteristics and comparisons with static behaviors are illustrated in Figures 18 and 19 as mean stress-time curves at several levels of total deformation and rupture to indicate the effect of stressing frequency on the high-temperature properties of type 321 stainless steel.

The extent to which the 1500°F cyclic deformation and rupture characteristics of the stainless steel alloy depend upon stress amplitude is clearly demonstrated in Figure 20 which represents the combinations of static mean tensile stress and alternating

tensile stress required to produce definite amounts of total deformation and rupture at the 20 and 100-hour time levels for the indicated frequencies of stress cycle applications.

Consistent with the manner of presenting the data for N-155 and Inconel X, the individual and combined influences of the cyclic stress variables on the 1500°F rupture behavior of 321 stainless steel can be expressed as a ratio of cyclic mean rupture stress to static rupture stress for rupture times up to 500 hours as compiled in Table 5 presented below.

TABLE 5

MEAN STRESS RATIOS TO PRODUCE RUPTURE OF TYPE 321 STAINLESS STEEL UNDER CYCLIC LOAD AS COMPARED TO STATIC LOAD

Temp. °F	Cyclic Stress Amplitude %	Cyclic Stress Frequency CPM	Ratio Cyclic Mean Rupture Stress to Static Rupture Stress 10 Hours	20 Hours	50 Hours	100 Hours	200 Hours	500 Hours
1500	± 25	11.5	0.91	0.89	0.84	0.81	0.76	0.77*
		115	1.10	1.06	1.00	1.02	1.04	1.10
		3,600	1.07	1.03	0.96	1.02	1.04	1.22
		14,400		0.91	0.88	0.84	0.80	
	± 67	115	0.87	0.84	0.85	0.88	0.88	0.92
		3,600	1.05	0.97	0.85	0.88	0.90	
		14,400	0.72	0.78	0.85	0.82	0.72	

*Ratio calculated from extrapolated stress values.

Through the range of rupture times involved, the ratios show that both slow and rapid cycling of the ± 25% stress amplitude results in rupture acceleration while the intermediate stressing frequencies of 115 and 3600 cycles per minute impart a delayed rupture effect. Under the influence of the ± 67% cyclic stress component however, with the exception of the 3600 cpm short-time behavior, rupture seems to be promoted regardless of stressing frequency.

The 1500°F data summarized in terms of stress and cycles to failure are compiled in Table 22. Graphical illustrations of the rupture characteristics on the basis of maximum stress and stress cycles applied are presented as S-N curves in Figure 21 for the entire frequency range from 11.5 to 14,400 cycles per minute. While the curves show that rupture for this alloy is primarily dependent upon time, the tendency of the 3600 and 14,400 cpm curves to converge at low stress values suggests a transition from time dependent to cyclic dependent failure.

At very low frequencies of cyclic stressing, it might be expected that an average or effective creep rate could be calculated by integrating the characteristic creep rates between the limits of minimum and maximum stress in the cycle. Such procedure was followed by Manjoine (4) for pulsating stresses superimposed upon various mean stresses at 1200 cycles per minute for 14S-T aluminum in the temperature range of 400°F. Under the conditions of testing, the measured rate of creep deformation was less than the rate determined by the calculation. These results, however, are not surprising, since investigations dealing with the effects of dynamic loads on the deformation properties of metals have shown that major changes can be produced over a range of strain rate.

As early as 1904, the influence of rapid loading on ultimate strength and plastic yielding was observed by Hopkinson (7) who found that iron and copper wires rapidly loaded in tension could be stressed beyond their static fracture stresses without exhibiting plastic yielding. More recently Clark (8), by means of tension-impact studies, has demonstrated that metals may take on entirely different strength and deformation characteristics depending on impact velocity. These findings are particularly significant because they illustrate the existence of dynamic as well as static stress-strain curves and the importance of the time element in the deformation process.

In tests where a metal is subjected to direct positive stressing such as encountered in pull-pull tests, the frequency of the applied cyclic stress as well as its amplitude will control the dynamic loading rate which the metal experiences during each cycle. At low temperatures, such application of cyclic stress usually leads to a type of failure termed "fatigue" which is considered to be a cyclic-dependent phenomenon although it has been shown that the rate of stress cycling will alter the stress vs. cycles to failure relationships of metals, particularly at high stress levels (9). If under similar cyclic stress conditions, metals are exposed to elevated temperatures, then progressive damage and ultimate failure will occur by creep, fatigue or a combination of both.

For the particular load boundaries of concern in this study, wherein a continuously fluctuating tensile load exists, the time-dependent phenomena controlling the plastic flow damage have been found to be the predominating factors in determining failure time. This is true not only because of the continuous creep that might be considered to be associated with a net effective tensile stress but also because of the time-dependent plastic flow that accumulates during each load cycle. The latter portion of the total creep damage

generated by the individual stress cycles would be expected to be related to the frequency of the fluctuating load component inasmuch as this variable regulates the time for plastic flow to initiate or accumulate during each cycle.

Results obtained under the present investigation have permitted some correlations to be made of the cyclic stress variables with failure life and rate of creep for the test alloys at elevated temperatures. Figures 22 and 23 attempt to illustrate schematically the trend of these results and suggest the likelihood of a dual mechanism varying in intensity for promoting failure over the full frequency spectrum. At low frequencies, creep, under the combined static and fluctuating loads is relatively rapid but decreases as frequency is increased. This behavior is to be expected, not only on the basis of the dynamic stress-strain behaviors of metals, but also, because less time becomes available in a single cycle for the initiation of metal flow or slip. Extending this reasoning to even higher frequencies, it might be expected that the rate of creep deformation would diminish to a value characteristic of the minimum stress in the cycle.

At sufficiently high frequencies, accelerated failure, accompanied by rapid creep deformation has been encountered. It is quite likely that the damaging mechanism associated with this high frequency effect is a cycle-dependent one, since only at these high frequencies of stressing are adequate numbers of cycles accumulated in the times under consideration to make its influence apparent. However, the cycle-dependent damage affect, regardless of its basic nature, manifests itself as accelerated creep. These same general trends which have been defined in reference to Figure 22 may be applied to the failure time vs. frequency chart presented in Figure 23.

It can be further reasoned that the schematic curves illustrated in Figures 22 and 23 will be displaced either to the right or left along the frequency axis as temperature is raised or lowered respectively. With increases in temperature, creep occurs at faster rates necessitating faster stressing frequencies to suppress the creep deformation to that characteristic of the minimum stress in the cycle. In addition, it is quite likely that amplitude increases could shift the cycle-dependent high frequency end of the curve to the left as a consequence of intensifying the cycle-dependent damage imparted in each cycle.

In keeping with the analysis which has been advanced as an explanation to account for the effects on creep and rupture associated with the variables of high-temperature cyclic stressing, Figures 24 through 28 have been prepared, from actual test data on the test alloys, to illustrate deformation and rupture times as a

function of stressing frequency. It becomes immediately apparent from these relationships, particularly for N-155 and type 321 stainless steel, that optimum frequencies of stressing exist for which the combined portions of time-dependent and cycle-dependent damage are a minimum, and for which the alloys exhibit their greatest resistances to flow and rupture. Thus, to cite a specific case for rupture of N-155 at 1500°F, it is seen from Figure 25 that a cyclic stress, with amplitude of 25% of the mean stress, prolongs the rupture life, relative to the static mean stress life in the frequency range of 30 to 7000 cycles per minute. At frequencies lower than 30 cpm, the rupture time would be expected to decrease to a value characteristic of the static rupture time associated with the maximum stress in the cycle. At frequencies higher than 7000 cpm, rupture time is dropping rapidly as a result of the predominant cycle-dependent damage.

The results obtained for Inconel X, as shown in Figures 26 and 27, indicate that significant cyclic-dependent damage has not occurred for the conditions shown even at the highest frequency of cyclic load investigated. For this alloy at 1350 and 1500°F, a wider range of frequency would have to be investigated in order to display the dome-shaped trend of rupture time versus frequency.

Associated with the delayed and accelerated creep and rupture effects displayed by the cyclically loaded test alloys, certain generalizations present themselves regarding ductility as determined by rupture elongation. Inasmuch as stress and time constitute the important factors regulating high-temperature ductility, one or the other of these variables is best applied as a basis by which ductilities under static and cyclic load conditions may be compared. For various mean stress values, the effects induced by the frequency of cyclic stressing for the ± 25 and 67% stress amplitudes on the test alloys at 1350 and 1500°F are illustrated in Figures 29 through 34. Under the influence of the ± 25 and 67% cyclic stress components, various trends in rupture ductility appear to exist at the 1350 and 1500°F temperature levels. For the ± 25% amplitude condition, for example, N-155 at the low end of the frequency spectrum and 1500°F experiences a loss in ductility relative to that characteristic of mean static stress. Rupture elongation appears to be gradually restored and eventually slightly exceeds the static ductility as stressing frequency is increased. On the other hand, type 321 stainless steel for both the ± 25 and 67% amplitude series at 1500°F exhibits a trend toward improved ductility at the low and high ends of the frequency scale but normal ductility at intermediate frequencies. N-155 exposed to the ± 25% cyclic stress at 1350°F displays a gradual reduction in ductility with increasing frequency while ductility of Inconel X under similar conditions of stressing at 1350 and 1500°F is essentially unaffected up to the 3600 cpm level

but is reduced thereafter. Both N-155 and Inconel X exposed to the ± 67% cyclic stress component display reduced rupture ductilities in the entire frequency range at 1350 and 1500°F.

With the exception of the ± 67% series of tests which in general show accelerated damage and rupture with corresponding losses in ductility, it appears that for those conditions of stressing where delayed rupture has been observed, the test alloys exhibit reduced ductilities which may be indicative of the existence of a cyclic-dependent mechanism in promoting rupture.

From the results obtained to date, no evidence is available to account for the accelerated creep and decreased rupture time resulting from cyclic tensile stresses of relatively high frequency. No difficulty was encountered in controlling the temperature of the sheet test specimens as indicated by the insulated thermocouples attached to their surface. If internal heating were significant then accelerated creep behavior should have been demonstrated by the Inconel X at the 14,400 cpm frequency. Although metallographic differences were not noticeable between statically and dynamically loaded creep test specimens, it is possible that microstructural instabilities are responsible for the cycle-dependent creep and rupture behavior noted for the high frequency load condition.

SUMMARY AND CONCLUSIONS

1. The equipment designed for high-temperature creep-rupture study under dynamic stressing provides a very suitable method of evaluating the effects of fluctuating tensile stresses over a range of frequencies and cyclic stress amplitudes. For low frequency tests (11.5 and 115 cycles per minute) conventional lever-type tensile-creep machines were modified to accommodate the superposition of a cyclic stress on the test specimen through a spring actuated by a motor driven eccentric. High frequency tests employed an electromagnetic vibrator driving a tuned mechanical system to develop the desired cyclic stress conditions. Both types of equipment incorporated load control and load measuring instrumentation to permit desired stress patterns to be maintained over long periods of time.

2. The effects of frequency and amplitude of cyclic stressing at constant temperature were demonstrated by presenting a series of mean stress-time curves for varying frequency at fixed stress amplitude and mean stress-alternating stress curves at fixed frequencies which can be compared with suitable static creep-rupture characteristics.

3. On the basis of the results obtained for the three test alloys subjected to cyclic loads at constant temperature, a variety of creep-rupture behaviors exists ranging from pronounced acceleration in creep and rupture to delayed creep and rupture, depending upon the magnitude of the mean load and stress amplitude and frequency of the cyclically applied load.

4. When superimposed cyclic stresses are applied at rates of 115 and 3600 cycles per minute, it is observed that a superimposed ± 25% stress amplitude has no appreciable effect on the static creep rupture behavior of low carbon N-155 at 1350°F. At 1500°F there is a delay in rupture induced by the ± 25% stress amplitude for this alloy.

5. Under the influence of the ± 25% cyclic stress amplitude superimposed at the 115 and 3600 cycle per minute frequencies, Inconel X does not appear to be affected in its static creep and rupture behavior at either the 1350 or 1500°F temperature levels.

6. Cyclic stress components of ± 25% applied at frequencies of 115 and 3600 cycles per minute on type 321 stainless steel result in improvements in rupture behavior of the alloy at 1500°F.

7. For N-155 at 1350 and 1500°F and type 321 stainless steel at 1500°F there is an accelerated damage generated by the superposition of the ± 25% cyclic component at test frequencies of 11.5 and 14,400 cycles per minute. The amount of damage tends to become more pronounced at low stress values and long test times.

8. Through the entire range of frequencies, there is in general, accelerated rupture associated with the test alloys for the superposition of ± 67% cyclic stress amplitudes at the 1350 and 1500°F temperature levels. Inconel X at 1350°F for shorter times to rupture or high stresses shows a tendency to retard rupture under the action of the ± 67% cyclic component at 3600 cycles per minute.

9. Because of the variety of effects which can be induced by cyclic stressing on the high-temperature creep and rupture properties of alloys, it appears that limiting stress values for use in design cannot be assigned to members undergoing vibratory type loading on the basis of data determined under static conditions. Instead, it seems that the effects on creep and rupture must be well defined for the specific conditions of cyclic stress amplitude and stressing frequency, and these results used for guidance in the assignment of stress values.

10. The high-temperature creep and fracture behavior of metals subjected to cyclic loads superimposed upon mean tensile loads, is influenced by two distinguishable mechanisms whose relative importance varies with the frequency of the dynamic load component. At low frequencies, creep rates and rupture times approach those values characteristic of the maximum stresses in the cycle while as frequency increases creep and rupture behavior approach asymptotically that equivalent to the minimum stress in the cycle. At the high frequency end of the scale an additional cycle-dependent damage effect occurs which accelerates failure.

11. The superposition of cyclic stress upon static tensile stress can induce a variety of rupture ductility effects at elevated temperatures. The test alloys, except for type 321 stainless steel which is essentially unaffected in its rupture elongation, show a trend of reduced ductility associated with the superposition of a ± 67% cyclic component and increasing frequency. Under the influence of a ± 25% cyclic component, trends ranging from reduced to improved ductility have been observed depending on the type of alloy, test temperature and frequency of the superimposed cyclic stress.

BIBLIOGRAPHY

1. American Society for Testing Materials "Symposium on Effect of Cyclic Heating and Stressing on Metals at Elevated Temperatures", ASTM Special Technical Publication No. 165, 17 June 1954.

2. Guarnieri, G. J., "High Temperature Sheet Studies" United States Navy Project SQUID, Technical Memorandum No. CAL-25, Report of Conference on Sheet Materials for Jet Propulsion Engines, 17 and 18 November 1948.

3. Lazan, B. J., "Dynamic Creep and Rupture Properties of Temperature Resistant Materials Under Tensile Fatigue Stresses", Proceedings American Society for Testing Materials, Vol. 49, 1949, pp. 757-787.

4. Manjoine, M. J., "Effect of Pulsating Loads on the Creep Characteristics of Aluminum Alloy 14S-T", Proceedings American Society for Testing Materials, Vol. 49, 1949, pp. 788-798.

5. Gillig, F. J. and Guarnieri, G. J., "Cyclic Loading Effects on the Creep Properties of Sheet Materials", United States Navy and Air Force Project SQUID, Technical Memorandum No. CAL-38, 28 September 1951.

6. Gillig, F. J., Guarnieri, G. J., and Yerkovich, L. A., "Apparatus for Conducting High Temperature Creep Studies Under Dynamic Load Conditions", First International Instrument Congress of the Instrument Society of America, Paper No. 54-25-2, September 20, 1954.

7. Hopkinson, B., "The Effect of Momentary Stresses in Metals" Proceedings Royal Society, Vol. 74, 1904-5, p. 498.

8. Clark, D. S., "The Behavior of Metals Under Dynamic Loading", Trans. American Society for Metals, Vol. 46, 1954, pp. 34-62.

9. Mann, J. Y., "The Effect of Rate of Cycling on the Fatigue Properties of 24S-T Aluminum Alloy", Commonwealth of Australia, Department of Supply, Aeronautical Research Laboratories Report SM.188, August 1954.

TABLE 6

CONSTANT LOAD-CONSTANT TEMPERATURE TEST DATA FOR LOW CARBON N-155 SHEET, AS-RECEIVED

Temp. °F	Stress PSI	Time in Hours for Total Deformation of 0.2%	1.0%	2.0%	5.0%	Fracture	Time of Test Hours	% Elongation in 2 In.	Minimum Creep Rate % Per Hour	Specimen
1350	26,000	3.50	39.75	75.50	142.40	194.25	194.25	10.00	0.022	118-7
	28,000	1.10	18.80	38.00	68.00	107.00	107.00	14.00	0.045	118-27
	30,000	0.60	12.50	29.00	54.40	77.25	77.25	9.00	0.055	118-1
	35,000	*	2.70	9.35	23.25	28.50	28.50	8.50	0.150	118-29
	40,000	*	*	0.05		2.25	2.25	5.00	0.620	118-2
1500	13,000	3.70	217.25	390.40	630.50	766.00	766.00	10.50	0.0017	118-140
	15,000	1.70	82.60	147.00		200.00	200.00	6.00	0.010	118-6
	17,000	1.15	12.00	30.55	62.25	82.75	82.75	10.50	0.054	118-30
	19,000	0.40	3.25	10.00	24.50	42.30	42.30	12.00	0.148	118-8
	21,000	0.30	1.60	4.20	10.65	20.50	20.50	15.00	0.385	118-38
	24,000	0.10	0.75	1.65	3.90	5.00	5.00	17.00	1.111	118-9

* Deformation obtained on loading.

TABLE 7

CYCLIC LOAD TEST DATA FOR LOW CARBON N-155 SHEET, AS-RECEIVED

Temp. °F	Dynamic Stress: Frequency CPM	Dynamic Stress: Amplitude % of Mean Stress	Mean Stress PSI	Time in Hours for Total Deformation of: 0.2%	1.0%	2.0%	5.0%	Fracture	Time of Test Hours	% Elong. in 2 In.	Min. Creep Rate % Per Hour	Specimen
1500	11.5	25.8	10,000	22.25	Test Discontinued				551.75	0.40	0.0002	118-158
	11.5	26.9	13,000	2.95	183.50	351.00	581.00	607.75	607.75	6.00	0.0036	118-181
	11.5	26.9	15,000	2.20	41.85	75.25		120.25	120.25	4.00	0.0118	118-177
	11.5	27.4	17,000	0.45	13.50	26.45	52.90	57.00	57.00	7.00	0.0496	118-178
	11.5	26.6	19,000	0.30	3.15	7.55	18.40	28.25	28.25	8.00	0.2050	118-157

TABLE 8

CYCLIC LOAD TEST DATA FOR LOW CARBON N-155 SHEET, AS-RECEIVED

Temp. °F	Dynamic Stress: Frequency CPM	Dynamic Stress: Amplitude % of Mean Stress	Mean Stress PSI	Time in Hours for Total Deformation of: 0.2%	1.0%	2.0%	5.0%	Fracture	Time of Test Hours	% Elong. in 2 In.	Min. Creep Rate % Per Hour	Specimen
1350	115	24.7	26,000	1.10	32.75	66.00	121.50	138.00	138.00	7.50	0.0253	118-34
	"	23.4	28,000	*	15.75	36.40	76.65	96.00	96.00	9.50	0.0410	118-35
	"	23.6	30,000	0.05	9.45	28.00	52.35	59.50	59.50	8.00	0.0539	118-39
	"	24.3	35,000	*	0.10	0.25	29.90	34.00	34.00	6.50	0.1012	118-41
	"	29.9	36,800	*	*	*	8.25	9.75	9.75	6.00	0.1800	118-42
1350	115	67.5	18,000	3.40	179.50	508.00		545.00	545.00	2.00	0.0030	118-152
	"	68.2	20,000	*	51.90	117.20		137.25	137.25	3.50	0.0153	118-53
	"	66.6	22,000	*	33.35	83.30		112.25	112.25	3.00	0.0189	118-54
	"	68.5	26,000	*	*	7.00		8.75	8.75	3.50	0.0467	118-51
	"	65.7	30,000	*	*	*		2.10	2.10	6.00	0.2800	118-52
1500	115	25.4	13,000	2.40	165.00	302.00	500.00	572.00	572.00	8.50	0.0023	118-68
	"	22.4	15,000	1.90	58.00	123.25	234.25	346.75	346.75	14.50	0.0143	118-37
	"	26.7	17,000	0.60	10.65	29.10	79.50	92.50	92.50	10.00	0.0542	118-31
	"	28.5	19,000	0.40	4.65	12.65	28.35	41.50	41.50	10.00	0.1250	118-36
	"	25.7	21,000	0.15	1.75	4.30	10.10	14.00	14.00	10.50	0.3921	118-32
	"	25.4	24,000	0.10	0.95	1.95	4.40	7.00	7.00	11.00	0.9412	118-33
1500	115	65.0	13,000	3.65	81.50	145.50	243.00	261.25	261.25	7.00	0.0088	118-136
	"	67.8	15,000	0.90	39.00	71.75		95.10	95.10	5.00	0.0210	118-43
	"	66.2	17,000	0.95	14.55	28.80		29.75	29.75	4.00	0.0588	118-46
	"	67.2	19,000	0.25	2.50	6.05		13.00	13.00	4.50	0.2820	118-49
	"	66.0	21,000	0.05	1.05	2.50		4.75	4.75	4.00	0.8000	118-47
	"	65.3	24,000	*	0.05	0.10	0.35	0.90	0.90	9.50	12.0000	118-48

*Deformation obtained on loading, mean stress and amplitude adjustment.

TABLE 9

CYCLIC LOAD TEST DATA FOR LOW CARBON N-155 SHEET, AS-RECEIVED

Temp. °F	Dynamic Stress: Frequency CPM	Dynamic Stress: Amplitude % of Mean Stress	Mean Stress PSI	Time in Hours for Total Deformation of: 0.2%	1.0%	2.0%	5.0%	Fracture	Time of Test Hours	% Elong. in 2 In.	Min. Creep Rate % Per Hour	Specimen
	3600	25.0	26,000	*	40.15	74.60		131.00	131.00	4.50	0.0162	118-63
	3600	25.0	28,000	*	30.50	61.00	109.75	112.50	112.50	5.50	0.0328	118-57
1350	3600	25.0	30,000	*	15.35	33.20	63.20	68.25	68.25	6.00	0.0560	118-60
	3600	25.0	35,000	*	*	2.85	21.25	21.25	21.25	5.00	0.1000	118-62
	3600	25.0	40,000	*	*	*		4.50	4.50	4.00		118-64
	3600	67.0	18,000	2.85	695.00(a)			(b)	642.00	0.93	0.0009	118-145
	3600	67.0	20,000	15.90	163.20			(c)	279.50	1.62	0.0054	118-77
1350	3600	67.0	22,000	6.25	(d)			379.50	379.50	6.00		118-171
	3600	67.0	24,000	(d)				156.50	156.50	6.50		118-167
	3600	67.0	26,000	(d)				59.50	59.50	3.50		118-169
	3600	25.0	15,000	1.60	70.10	131.50	256.70	292.50	292.50	9.50	0.0117	118-65
	3600	25.0	17,000	0.15	13.30	36.60	79.05	92.75	92.75	7.50	0.0429	118-67
1500	3600	25.0	19,000	0.25	5.25	11.30	24.35	44.00	44.00	19.00	0.1600	118-69
	3600	25.0	21,000	*	2.50	7.15		26.50	26.50	10.00	0.2150	118-70
	3600	25.0	24,000	*	0.90	1.85	4.75	7.60	7.60	14.00	1.0345	118-71
	3600	67.0	13,000	6.50	118.50			221.50	221.50	5.00	0.0046	118-139
	3600	67.0	15,000					118.50	118.50	4.50		118-76
1500	3600	67.0	17,000	0.05	13.00	36.00	54.60	67.50	67.50	5.50	0.0443	118-137
	3600	67.0	19,000	0.20	6.05			12.00	12.00	2.50	0.0843	118-141
	3600	67.0	21,000	*	2.85			3.75	3.75	1.50	0.3230	118-142

* Deformation obtained on loading, mean stress and amplitude adjustment.
(a) Extrapolated value from time-deformation curve.
(b) Specimen did not fracture - test discontinued.
(c) Specimen fractured at pin joint by fatigue.
(d) Creep measuring extensometers slipped.

TABLE 10

CYCLIC LOAD TEST DATA FOR LOW CARBON N-155 SHEET, AS-RECEIVED

Temp. °F	Dynamic Stress: Frequency CPM	Dynamic Stress: Amplitude % of Mean Stress	Mean Stress PSI	Time in Hours for Total Deformation of: 0.2%	1.0%	2.0%	5.0%	Fracture	Time of Test Hours	% Elong. in 2 In.	Min. Creep Rate % Per Hour	Specimen
	14,400	25.0	18,000	0.50	76.50	194.75	357.90	584.50	584.50	7.00	0.0049	118-176
1350	"	25.0	21,000	1.35	35.00	77.00	137.75	143.75	143.75	5.50	0.0185	118-175
	"	25.0	24,000	*	14.90	45.50	84.20	112.25	112.25	6.50	0.0276	118-174
	"	25.0	28,000	*	1.85	11.30		29.00	29.00	4.50	0.0900	118-173
	14,400	25.0	10,000	1.65	230.00	410.25	675.00(a)	777.00	777.00	9.00	0.0021	118-172
	"	25.0	13,000	0.50	41.70	87.30	161.90	221.25	221.25	10.50	0.0125	118-166
1500	"	25.0	15,000	0.50	5.15	25.00	52.40	114.50	114.50	13.50	0.0425	118-168
	"	25.0	17,000	0.10	4.60	11.85	26.75	32.75	32.75	7.00	0.1400	118-165
	"	25.0	19,000	0.05	1.10	2.85	7.15(a)	17.25	17.25	14.50	0.5225	118-170

*Deformation obtained on loading, mean stress and amplitude adjustment.
(a) Extrapolated value from time-deformation curve.

TABLE 11

DIRECT POSITIVE STRESS FATIGUE DATA FOR LOW CARBON N-155, AS-RECEIVED

Temp. °F	Dynamic Stress: Frequency CPM	Dynamic Stress: Amplitude % of Mean Stress	Mean Stress PSI	Alternating Stress PSI	Maximum Stress PSI	Cycles to Failure x 10^6	Specimen
	115	24.7	26,000	6,425	32,425	0.952	118-34
	115	23.4	28,000	6,550	34,550	0.662	118-35
1350	115	23.6	30,000	7,080	37,080	0.410	118-39
	115	24.3	35,000	8,500	43,500	0.235	118-41
	115	29.9	36,800	11,000	47,800	0.067	118-42
	3,600	25.0	26,000	6,500	32,500	28.30	118-63
	3,600	25.0	28,000	7,000	35,000	24.30	118-57
1350	3,600	25.0	30,000	7,500	37,500	14.74	118-60
	3,600	25.0	35,000	8,750	43,750	4.59	118-62
	3,600	25.0	40,000	10,000	50,000	0.97	118-64
	14,400	25.0	18,000	4,500	22,500	505.0	118-176
1350	14,400	25.0	21,000	5,250	26,250	124.2	118-175
	14,400	25.0	24,000	6,000	30,000	97.0	118-174
	14,400	25.0	28,000	7,000	35,000	25.1	118-173
	115	67.5	18,000	12,150	30,150	3.760	118-152
	115	68.2	20,000	13,640	33,640	0.947	118-53
1350	115	66.6	22,000	14,650	36,650	0.774	118-54
	115	68.5	26,000	17,810	43,810	0.060	118-51
	115	65.7	30,000	19,710	49,710	0.014	118-52
	3,600	67.0	18,000	12,060	30,060	>138.7	118-145
	3,600	67.0	20,000	13,400	33,400	> 60.4	118-77
1350	3,600	67.0	22,000	14,740	36,740	81.9	118-171
	3,600	67.0	24,000	16,080	40,080	33.8	118-167
	3,600	67.0	26,000	17,420	43,420	12.9	118-169

TABLE 11 (Contd.)

DIRECT POSITIVE STRESS FATIGUE DATA FOR LOW CARBON N-155, AS-RECEIVED

Temp. °F	Dynamic Stress: Frequency CPM	Dynamic Stress: Amplitude % of Mean Stress	Mean Stress PSI	Alternating Stress PSI	Maximum Stress PSI	Cycles to Failure x 10^6	Specimen
	11.5	25.8	10,000	2,580	12,580	>0.381	118-158
	11.5	26.9	13,000	3,500	16,500	0.419	118-181
1500	11.5	26.9	15,000	4,035	19,035	0.083	118-177
	11.5	27.4	17,000	4,660	21,660	0.039	118-178
	11.5	26.6	19,000	5,055	24,055	0.019	118-157
	115	25.4	13,000	3,300	16,300	3.95	118-68
	115	22.4	15,000	3,360	18,360	2.39	118-37
1500	115	26.7	17,000	4,540	21,540	0.64	118-31
	115	28.5	19,000	5,415	24,415	0.29	118-36
	115	25.7	21,000	5,400	26,400	0.10	118-32
	115	25.4	24,000	6,100	30,100	0.05	118-33
	3,600	25.0	15,000	3,750	18,750	63.18	118-65
	3,600	25.0	17,000	4,250	21,250	20.04	118-67
1500	3,600	25.0	19,000	4,750	23,750	9.51	118-69
	3,600	25.0	21,000	5,250	26,250	6.73	118-70
	3,600	25.0	24,000	6,000	30,000	1.03	118-71
	14,400	25.0	10,000	2,500	12,500	671.3	118-172
	14,400	25.0	13,000	3,250	16,250	191.2	118-166
1500	14,400	25.0	15,000	3,750	18,750	98.9	118-168
	14,400	25.0	17,000	4,250	21,250	28.3	118-165
	14,400	25.0	19,000	4,750	23,750	14.9	118-170
	115	65.0	13,000	8,450	21,450	1.800	118-136
	115	67.8	15,000	10,170	25,170	0.656	118-43
1500	115	66.2	17,000	11,250	28,250	0.205	118-46
	115	67.2	19,000	12,770	31,770	0.090	118-49
	115	66.0	21,000	13,860	34,860	0.033	118-47
	115	65.3	24,000	15,675	39,675	0.006	118-48

TABLE 11 (Contd.)

DIRECT POSITIVE STRESS FATIGUE DATA FOR LOW CARBON N-155, AS-RECEIVED

Temp. °F	Dynamic Stress: Frequency CPM	Dynamic Stress: Amplitude % of Mean Stress	Mean Stress PSI	Alternating Stress PSI	Maximum Stress PSI	Cycles to Failure x 10^6	Specimen
	3,600	67.0	13,000	8,710	21,710	47.85	118-139
	3,600	67.0	15,000	10,050	25,050	25.60	118-76
1500	3,600	67.0	17,000	11,390	28,390	14.59	118-137
	3,600	67.0	19,000	12,730	31,730	2.60	118-141
	3,600	67.0	21,000	14,070	35,070	0.82	118-142

TABLE 12

CONSTANT LOAD-CONSTANT TEMPERATURE TEST DATA FOR AGED INCONEL X SHEET

Temp. °F	Stress PSI	Time in Hours for Total Deformation of 0.1%	0.2%	0.5%	1.0%	Fracture	Time of Test Hours	% Elongation in 2 In.	Minimum Creep Rate % Per Hour	Specimen
1350	32,000	2.15	17.25	87.50	147.75	152.00	152.00	2.50	0.0043	155-49
	35,000	*	1.60	43.00	79.70	118.00	118.00	3.00	0.0072	155-42
	40,000	*	0.70	18.70	34.00	43.50	43.50	2.00	0.0169	155-41
	45,000	*	0.45	6.35	13.60	15.75	15.75	1.50	0.0690	155-40
	50,000	*	*	1.35	3.85	4.80	4.80	2.00	0.2000	155-48
1500	13,000	4.05	19.50	69.85	133.10	222.50	222.50	3.00	0.0055	155-53
	16,000	3.70	14.50	39.10	66.65	104.00	104.00	3.00	0.0093	155-45
	18,000	1.55	7.10	27.90	52.40	92.00	92.00	4.00	0.0145	155-43
	20,000	1.65	5.50	19.70	39.10	63.00	63.00	3.50	0.0211	155-37
	25,000	0.20	0.80	5.40	11.95	20.50	20.50	3.00	0.0652	155-38
	30,000	*	0.05	0.30	0.90	3.00	3.00	4.50	0.8333	155-36

*Deformation obtained on loading.

TABLE 13

CYCLIC LOAD TEST DATA FOR AGED INCONEL X SHEET

Temp. °F	Dynamic Stress: Frequency CPM	Dynamic Stress: Amplitude % of Mean Stress	Mean Stress PSI	Time in Hours for Total Deformation of: 0.1%	0.2%	0.5%	1.0%	Fracture	Time of Test Hours	% Elong. in 2 In.	Min. Creep Rate % Per Hour	Specimen
	115	26.4	32,000	*	4.25	72.50	137.50	164.50	164.50	2.00	0.0044	155-1
	"	23.7	35,000	*	3.80	44.00	74.90	88.75	88.75	2.00	0.0075	155-2
1350	"	24.5	40,000	*	0.45	14.45	27.95	29.50	29.50	1.50	0.0214	155-3
	"	26.6	45,000	*	*	3.65	9.15	9.75	9.75	1.50	0.0671	155-4
	"	24.6	50,000	*	*	0.75	3.00	4.00	4.00	1.50	0.2222	155-5
	115	65.5	26,000	*	13.00	111.00	208.00(a)	(c)	175.25	0.81	0.0020	155-13
	"	68.0	28,000	*	8.70	81.70		124.00	124.00	1.50	0.0032	155-19
1350	"	67.5	30,000	*	4.10			56.00	56.00	0.50	0.0044	155-21
	"	66.6	32,000	*	3.60			20.50	20.50	1.00	0.0073	155-11
	"	70.3	35,000	*	1.40			8.75	8.75	1.00	0.0080	155-22
	115	25.0	16,000	2.50	7.95	44.00	86.80	127.50	127.50	2.50	0.0083	155-44
	"	26.3	18,000	2.05	8.95	26.40	49.00	74.75	74.75	2.50	0.0145	155-46
1500	"	26.2	20,000	0.90	3.80	16.20	30.85	57.75	57.75	5.00	0.0242	155-47
	"	23.9	25,000	*	0.65	3.95	9.10	17.00	17.00	3.50	0.0999	155-51
	"	26.5	30,000	*	*	0.45	1.30	4.10	4.10	5.50	0.5630	155-50
	115	66.0	13,000	1.95	7.50	42.50	115.00	160.50	160.50	1.50	0.0066	155-56
	"	67.6	16,000	1.75	7.90	26.10	46.00	53.50	53.50	2.00	0.0163	155-6
1500	"	67.8	18,000	0.75	4.30	15.85	25.60	36.75	36.75	2.50	0.0260	155-7
	"	65.0	20,000	0.35	1.40	4.65	9.45	10.00	10.00	1.50	0.0923	155-8
	"	66.5	25,000	*	0.10	0.85	2.10	3.25	3.25	2.00	0.4000	155-9
	"	68.6	30,000	*	*	*	0.10	0.40	0.40	3.50		155-10

* Deformation obtained on loading, mean stress and amplitude adjustment.
(a) Extrapolated value from time-deformation curve.
(c) Specimen fractured at pin joint by fatigue.

TABLE 14

CYCLIC LOAD TEST DATA FOR AGED INCONEL X SHEET

Temp. °F	Dynamic Stress: Frequency CPM	Dynamic Stress: Amplitude % of Mean Stress	Mean Stress PSI	Time in Hours for Total Deformation of: 0.1%	0.2%	0.5%	1.0%	Fracture	Time of Test Hours	% Elong. in 2 In.	Min. Creep Rate % Per Hour	Specimen
	3600	25.0	32,000	0.50	10.00	89.00		130.00	130.00	2.00	0.0025	155-29
	"	25.0	35,000	*	4.25	38.25	77.00	77.75	77.75	1.50	0.0063	155-30
1350	"	25.0	40,000	0.10	1.30	15.60		28.50	28.50	2.00	0.0142	155-31
	"	25.0	45,000	*	0.80	6.40	12.70	16.00	16.00	2.00	0.0380	155-34
	"	25.0	50,000	*	0.60	3.65		4.80	4.80	1.00	0.0890	155-32
	3600	67.0	26,000	2.75	39.90	165.30		227.25	227.25	1.00	0.0024	155-134
	"	67.0	28,000	0.30	2.85	61.20	168.50	186.00	186.00	1.25	0.0047	155-135
1350	"	67.0	30,000	(d)				(c)	70.00			155-132
	"	67.0	32,000	(d)				207.50	207.50	1.50		155-130
	"	67.0	35,000	(d)				140.00	140.00	1.00		155-129
	3600	25.0	16,000	*	3.60	29.90	59.70	117.25	117.25	4.00	0.0085	155-23
	"	25.0	18,000	1.20	4.20	27.00	55.10	74.50	74.50	3.00	0.0097	155-24
1500	"	25.0	20,000	0.60	3.50	14.50	27.80	43.75	43.75	3.50	0.0150	155-28
	"	25.0	25,000	*	*	4.60	11.30	16.25	16.25	4.00	0.0490	155-26
	"	25.0	30,000	*	*	0.45	1.50	4.00	4.00	5.00	0.4160	155-27
	3600	67.0	13,000	24.50	43.50	120.00		191.25	191.25	1.50	0.0039	155-121
	"	67.0	16,000	10.75	38.50			76.75	76.75	0.50	0.0078	155-123
1500	"	67.0	18,000	2.90	20.75	(d)		52.50	52.50	1.25		155-125
	"	67.0	20,000	0.10	2.75	(d)		43.00	43.00	2.00		155-128
	"	67.0	25,000	0.40	3.75	(d)		7.50	7.50	1.00		155-127

* Deformation obtained on loading, mean stress and amplitude adjustment.
(c) Specimen fractured at pin joint by fatigue.
(d) Creep measuring extensometers slipped.

TABLE 15

CYCLIC LOAD TEST DATA FOR AGED INCONEL X SHEET

Temp. °F	Dynamic Stress: Frequency CPM	Dynamic Stress: Amplitude % of Mean Stress	Mean Stress PSI	Time in Hours for Total Deformation of: 0.1%	0.2%	0.5%	1.0%	Fracture	Time of Test Hours	% Elong. in 2 In.	Min. Creep Rate % Per Hour	Specimen
	14,400	25.0	30,000	3.50	8.30	87.00		172.00	172.00	1.00	0.0036	155-140
1350	14,400	25.0	32,000	*	3.20	77.00	173.00	201.50	201.50	1.50	0.0037	155-141
	14,400	25.0	35,000	*	1.60	66.00	174.00	234.25	234.25	2.50	0.0042	155-142
	14,400	25.0	40,000					120.50	120.50	0.50		155-143
	14,400	25.0	13,000	2.60	12.30	77.50	153.80	224.50	224.50	3.00	0.0046	155-138
1500	14,400	25.0	16,000	1.85	8.50	39.20	85.00	111.50	111.50	1.50	0.0096	155-137
	14,400	25.0	18,000	0.80	6.00	18.30		34.75	34.75	1.50	0.0158	155-136
	14,400	25.0	20,000	0.50	7.00			18.25	18.25	0.50	0.0155	155-139

*Deformation obtained on loading, mean stress and amplitude adjustment.

TABLE 16

DIRECT POSITIVE STRESS FATIGUE DATA FOR AGED INCONEL X SHEET

Temp. °F	Dynamic Stress: Frequency CPM	Dynamic Stress: Amplitude % of Mean Stress	Mean Stress PSI	Alternating Stress PSI	Maximum Stress PSI	Cycles to Failure x 10^6	Specimen
	115	26.4	32,000	8,450	40,450	1.135	155-1
	115	23.7	35,000	8,300	43,300	0.613	155-2
1350	115	24.5	40,000	9,800	49,800	0.204	155-3
	115	26.5	45,000	11,920	56,920	0.067	155-4
	115	24.6	50,000	12,300	62,300	0.028	155-5
	3,600	25.0	32,000	8,000	40,000	28.08	155-29
	3,600	25.0	35,000	8,750	43,750	16.79	155-30
1350	3,600	25.0	40,000	10,000	50,000	6.16	155-31
	3,600	25.0	45,000	11,250	56,250	3.46	155-34
	3,600	25.0	50,000	12,500	62,500	1.04	155-52
	14,400	25.0	30,000	7,500	37,500	148.61	155-140
1350	14,400	25.0	32,000	8,000	40,000	174.10	155-141
	14,400	25.0	35,000	8,750	43,750	202.39	155-142
	14,400	25.0	40,000	10,000	50,000	104.11	155-143
	115	65.5	26,000	17,025	43,025	>1.210	155-13
	115	68.0	28,000	19,050	47,050	0.855	155-19
1350	115	67.5	30,000	20,250	50,250	0.387	155-21
	115	66.6	32,000	21,300	53,300	0.142	155-11
	115	70.3	35,000	24,600	59,600	0.060	155-22
	3,600	67.0	26,000	17,420	43,420	49.09	155-134
	3,600	67.0	28,000	18,760	46,760	40.18	155-135
1350	3,600	67.0	30,000	20,100	50,100	>15.12	155-132
	3,600	67.0	32,000	21,440	53,440	44.82	155-130
	3,600	67.0	35,000	23,450	58,450	30.24	155-129

TABLE 16 (Contd.)

DIRECT POSITIVE STRESS FATIGUE DATA FOR AGED INCONEL X SHEET

Temp. °F	Dynamic Stress: Frequency CPM	Dynamic Stress: Amplitude % of Mean Stress	Mean Stress PSI	Alternating Stress PSI	Maximum Stress PSI	Cycles to Failure x 10^6	Specimen
1500	115	25.0	16,000	4,000	20,000	0.880	155-44
	115	26.3	18,000	4,730	22,730	0.516	155-46
	115	26.2	20,000	5,240	25,240	0.398	155-47
	115	23.9	25,000	5,975	30,975	0.117	155-51
	115	26.5	30,000	7,950	37,950	0.028	155-50
1500	3,600	25.0	16,000	4,000	20,000	25.33	155-23
	3,600	25.0	18,000	4,500	22,500	16.09	155-24
	3,600	25.0	20,000	5,000	25,000	9.45	155-28
	3,600	25.0	25,000	6,250	31,250	3.51	155-26
	3,600	25.0	30,000	7,500	37,500	0.86	155-27
1500	14,400	25.0	13,000	3,250	16,250	193.97	155-138
	14,400	25.0	16,000	4,000	20,000	96.34	155-137
	14,400	25.0	18,000	4,500	22,500	30.03	155-136
	14,400	25.0	20,000	5,000	25,000	15.77	155-139
1500	115	66.0	13,000	8,580	21,580	1.105	155-56
	115	67.6	16,000	10,810	26,810	0.369	155-6
	115	67.8	18,000	12,200	30,200	0.254	155-7
	115	65.0	20,000	13,000	33,000	0.069	155-8
	115	66.5	25,000	16,620	41,620	0.023	155-9
	115	68.6	30,000	20,600	50,600	0.003	155-10
1500	3,600	67.0	13,000	8,710	21,710	41.31	155-121
	3,600	67.0	16,000	10,720	26,720	16.58	155-123
	3,600	67.0	18,000	12,060	30,060	11.34	155-125
	3,600	67.0	20,000	13,400	33,400	9.29	155-128
	3,600	67.0	25,000	16,750	41,750	1.62	155-127

TABLE 17

CONSTANT LOAD-CONSTANT TEMPERATURE TEST DATA FOR TYPE 321 STAINLESS STEEL SHEET, AS-RECEIVED

Temp. °F	Stress PSI	Time in Hours for Total Deformation of 0.2%	0.5%	1.0%	2.0%	4.0%	Fracture	Time of Test Hours	% Elong. in 2 In.	Min. Creep Rate % Per Hour	Specimen
1500	4,000	9.05	22.25	62.75	404.40		469.25	469.25	2.75	0.0013	142-81
	5,000	5.85	14.90	35.75			206.75	206.75	2.00	0.0015	142-83
	6,000	6.80	12.70	19.15	34.45	67.25	79.50	79.50	5.00	0.0198	142-80
	8,000	1.75	4.60	7.85	12.60	21.05	28.00	28.00	5.50	0.0762	142-79
	10,000	0.60	2.10	4.00	6.70	10.25	11.25	11.25	5.00	0.1995	142-82

TABLE 18

CYCLIC LOAD TEST DATA FOR TYPE 321 STAINLESS STEEL SHEET, AS-RECEIVED

Temp. °F	Dynamic Stress: Frequency CPM	Dynamic Stress: Amplitude % of Mean Stress	Mean Stress PSI	Time in Hours for Total Deformation of: 0.2%	0.5%	1.0%	2.0%	4.0%	Fracture	Time of Test Hours	% Elong. in 2 In.	Min. Creep Rate % Per Hour	Specimen
	11.5	24.2	4,000	6.50	11.75	23.30	49.00	129.90	177.25	177.25	8.50	0.0222	142-106
1500	11.5	26.5	5,000	4.10	11.00	20.25	37.00	68.40	73.00	73.00	5.00	0.0426	142-118
	11.5	26.7	6,000	1.75	4.40	7.90	14.30	28.30	48.50	48.50	9.00	0.0975	142-116
	11.5	26.9	8,000	1.00	2.65	4.90	8.15	13.30	18.25	18.25	7.00	0.1513	142-112

TABLE 19

CYCLIC LOAD TEST DATA FOR TYPE 321 STAINLESS STEEL SHEET, AS-RECEIVED

Temp. °F	Dynamic Stress: Frequency CPM	Dynamic Stress: Amplitude % of Mean Stress	Mean Stress PSI	Time in Hours for Total Deformation of: 0.2%	0.5%	1.0%	2.0%	4.0%	Fracture	Time of Test Hours	% Elong. in 2 In.	Min. Creep Rate % Per Hour	Specimen
	115	25.0	4,000	9.15	24.40	242.50			684.25	684.25	1.50	0.00036	142-87
	115	26.7	5,000	7.30	17.10	42.00			275.75	275.75	2.50	0.00116	142-85
1500	115	24.2	6,000	3.80	7.80	13.20	22.70	49.25	76.25	76.25	5.50	0.0560	142-84
	115	26.0	8,000	0.70	2.40	4.70	8.85	14.95	29.75	29.75	17.50	0.1840	142-86
	115	24.9	10,000	1.10	2.40	4.10	6.50	8.95	15.00	15.00	10.00	0.2083	142-88
	115	70.0	4,000	8.05	20.90	64.10	319.90		334.00	334.00	3.00	0.0027	142-89
	115	68.5	5,000	4.40	12.20	26.65	95.20		121.25	121.25	2.50	0.0098	142-90
1500	115	64.0	6,000	1.50	5.00	10.05	19.50	35.75	41.00	41.00	6.00	0.0937	142-91
	115	68.0	8,000	0.60	2.30	4.50	7.65	12.50	14.25	14.25	6.00	0.1945	142-92
	115	64.5	10,000	0.10	0.60	2.30	5.10	7.70	7.75	7.75	6.00	0.2820	142-93

TABLE 20

CYCLIC LOAD TEST DATA FOR TYPE 321 STAINLESS STEEL SHEET, AS-RECEIVED

Temp. °F	Dynamic Stress: Frequency CPM	Dynamic Stress: Amplitude % of Mean Stress	Mean Stress PSI	Time in Hours for Total Deformation of: 0.2%	0.5%	1.0%	2.0%	4.0%	Fracture	Time of Test Hours	% Elong. in 2 In.	Min. Creep Rate % Per Hour	Specimen
1500	3600	25.0	5,000	3.90	41.25				321.00	321.00	1.50	0.00072	142-95
	"	25.0	6,000	4.15	10.20	19.40	36.20		62.75	62.75	3.50	0.0255	142-101
	"	25.0	8,000	1.15	4.00	7.20	12.50	22.25	29.50	29.50	6.50	0.1130	142-102
	"	25.0	10,000	0.40	1.55	3.50	6.80		14.25	14.25	4.50	0.2360	142-97
1500	3600	67.0	5,000	4.15	11.10	25.00	64.15		117.75	117.75	2.50	0.0190	142-100
	"	67.0	6,000	3.05	6.00	10.20	18.15	34.30	42.75	42.75	5.50	0.0340	142-107
	"	67.0	8,000	0.85	2.50	4.80	8.50	15.25	24.75	24.75	8.50	0.1850	142-108
	"	67.0	10,000	1.10	2.40	4.10	6.65	10.25	12.25	12.25	7.00	0.1600	142-103

TABLE 21

CYCLIC LOAD TEST DATA FOR TYPE 321 STAINLESS STEEL SHEET, AS-RECEIVED

Temp. °F	Dynamic Stress: Frequency CPM	Dynamic Stress: Amplitude % of Mean Stress	Mean Stress PSI	Time in Hours for Total Deformation of: 0.2%	0.5%	1.0%	2.0%	4.0%	Fracture	Time of Test Hours	% Elong. in 2 In.	Min. Creep Rate % Per Hour	Specimen
1500	14,400	25.0	5,000	1.95	6.00	12.90	31.00		91.25	91.25	3.50	0.0217	142-99
	"	25.0	6,000	0.90	2.40	6.30	17.50	35.25	50.25	50.25	6.00	0.0772	142-104
	"	25.0	8,000	0.65	2.85	4.70	7.90	13.90	19.25	19.25	7.50	0.1260	142-110
	"	25.0	10,000	0.70	1.65	3.10	4.95	8.40	14.75	14.75	9.50	0.1980	142-111
1500	14,400	67.0	4,000	3.75	12.25	24.25	50.75		144.75	144.75	3.50	0.0168	142-114
	"	67.0	5,000	1.90	8.50	11.50	18.25		90.75	90.75	4.00	0.0268	142-119
	"	67.0	6,000	0.40	1.60	4.70	10.70	25.25	47.00	47.00	8.00	0.1280	142-109
	"	67.0	8,000	0.30	1.15	2.35	4.20		6.25	6.25	3.50	0.3430	142-113

TABLE 22

DIRECT POSITIVE STRESS FATIGUE DATA FOR TYPE 321 STAINLESS STEEL SHEET, AS-RECEIVED

Temp. °F	Dynamic Stress: Frequency CPM	Dynamic Stress: Amplitude % of Mean Stress	Mean Stress PSI	Alternating Stress PSI	Maximum Stress PSI	Cycles to Failure x 10^6	Specimen
1500	11.5	24.2	4,000	970	4,970	0.122	142-106
	11.5	26.5	5,000	1,325	6,325	0.050	142-118
	11.5	26.7	6,000	1,600	7,600	0.034	142-116
	11.5	26.9	8,000	2,150	10,150	0.013	142-112
1500	115	25.0	4,000	1,000	5,000	4.721	142-87
	115	26.7	5,000	1,335	6,335	1.902	142-85
	115	24.2	6,000	1,450	7,450	0.526	142-84
	115	26.0	8,000	2,080	10,080	0.205	142-86
	115	24.9	10,000	2,490	12,490	0.104	142-88
1500	3,600	25.0	5,000	1,250	6,250	69.336	142-95
	3,600	25.0	6,000	1,500	7,500	13.554	142-101
	3,600	25.0	8,000	2,000	10,000	6.372	142-102
	3,600	25.0	10,000	2,500	12,500	3.078	142-97
1500	14,400	25.0	5,000	1,250	6,250	78.840	142-99
	14,400	25.0	6,000	1,500	7,500	43.416	142-104
	14,400	25.0	8,000	2,000	10,000	16.632	142-110
	14,400	25.0	10,000	2,500	12,500	12.774	142-111
1500	115	70.0	4,000	2,800	6,800	2.305	142-89
	115	68.5	5,000	3,425	8,425	0.837	142-90
	115	64.0	6,000	3,840	9,840	0.283	142-91
	115	68.0	8,000	5,440	13,440	0.098	142-92
	115	64.5	10,000	6,450	16,450	0.054	142-93

TABLE 22 (Contd.)

DIRECT POSITIVE STRESS FATIGUE DATA FOR TYPE 321 STAINLESS STEEL SHEET, AS-RECEIVED

Temp. °F	Dynamic Stress: Frequency CPM	Dynamic Stress: Amplitude % of Mean Stress	Mean Stress PSI	Alternating Stress PSI	Maximum Stress PSI	Cycles to Failure x 10^6	Specimen
	3,600	67.0	5,000	3,350	8,350	25.434	142-100
1500	3,600	67.0	6,000	4,020	10,020	9.234	142-107
	3,600	67.0	8,000	5,360	13,360	5.346	142-108
	3,600	67.0	10,000	6,700	16,700	2.646	142-103
	14,000	67.0	4,000	2,680	6,680	125.064	142-114
1500	14,400	67.0	5,000	3,350	8,350	78.408	142-119
	14,400	67.0	6,000	4,020	10,020	40.608	142-109
	14,400	67.0	8,000	5,360	13,360	5.400	142-113

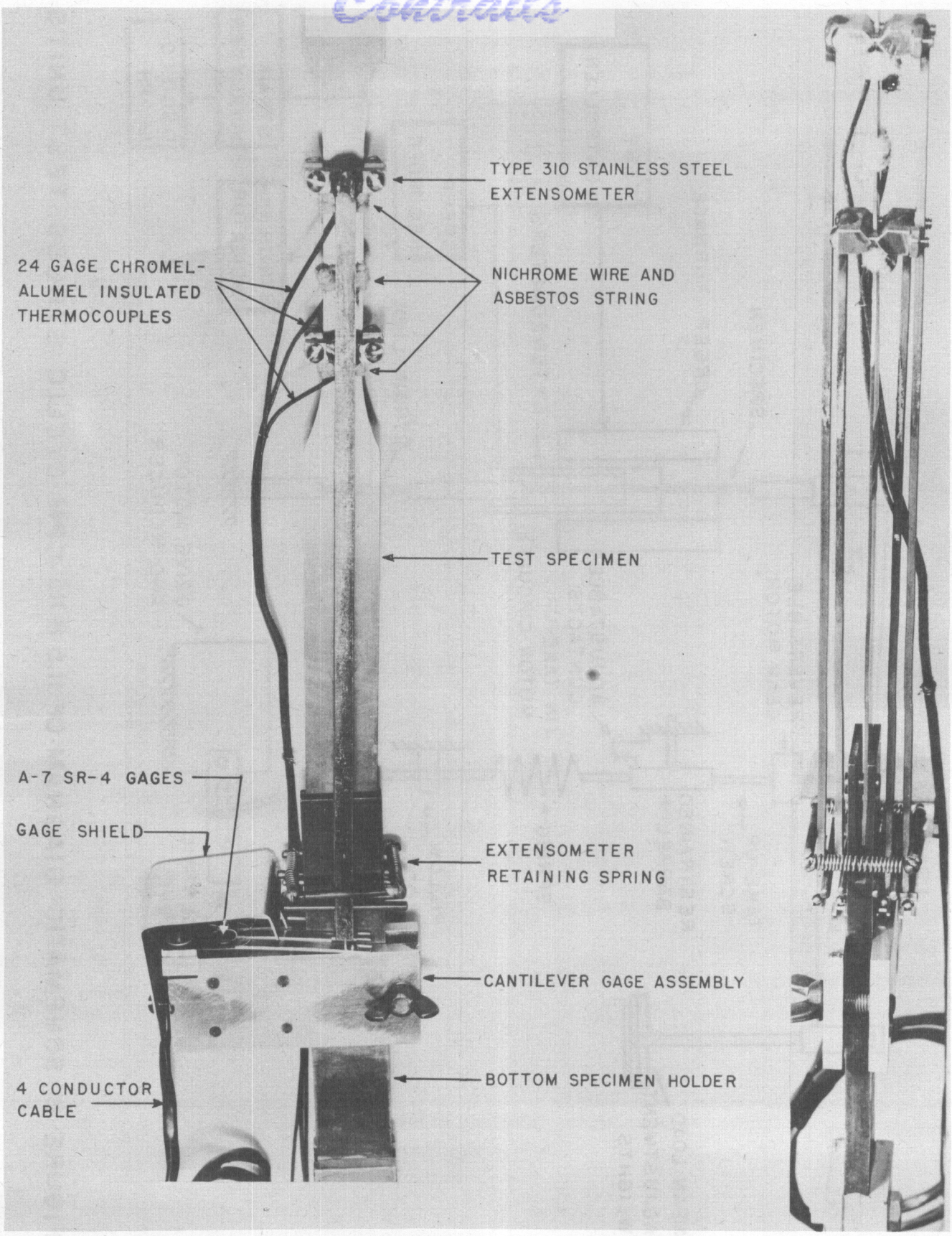

FIGURE 1 SPECIMEN - EXTENSOMETER - THERMOCOUPLE ASSEMBLY

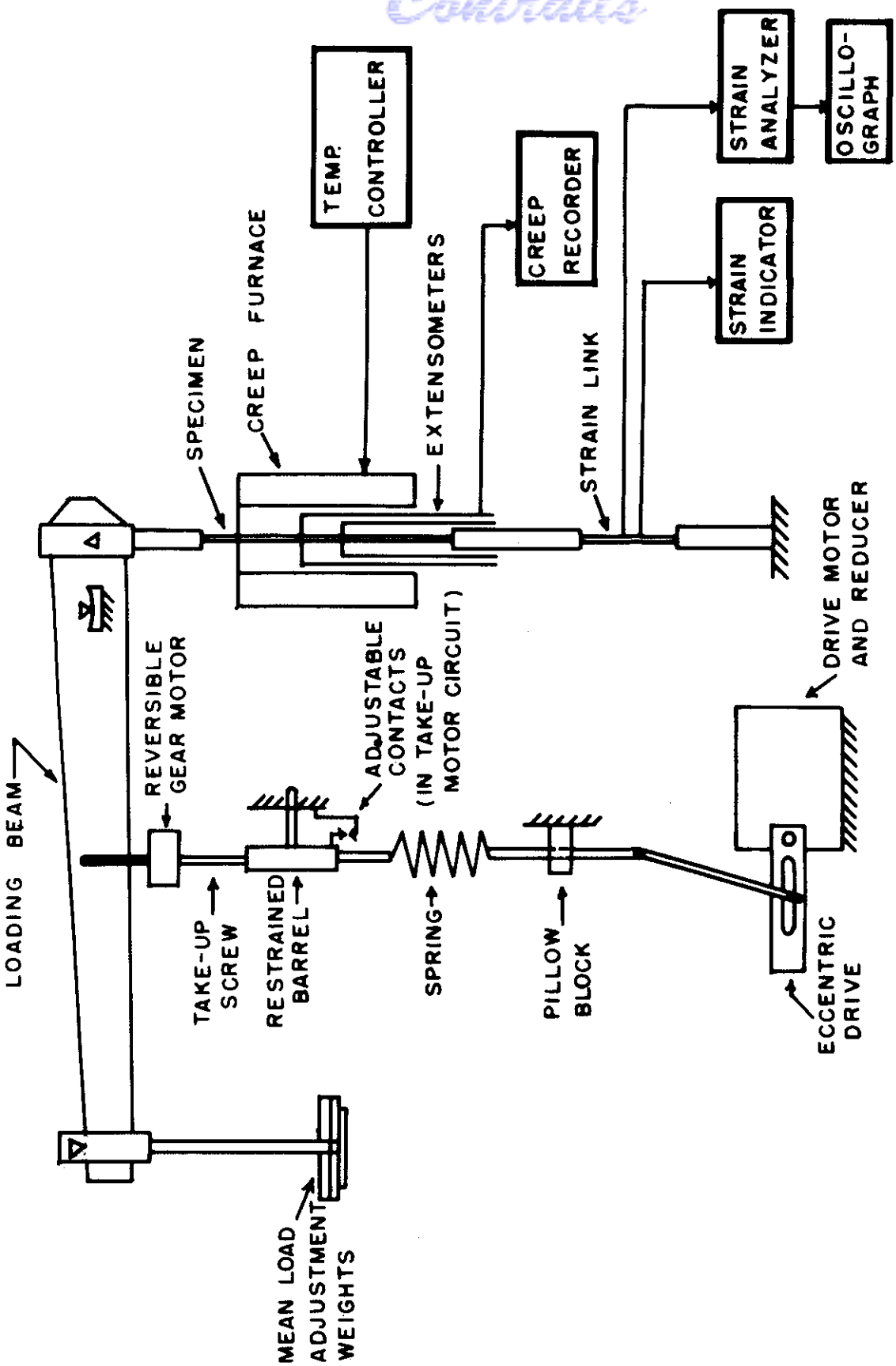

FIGURE 2 SCHEMATIC DIAGRAM OF 11.5 & 115 CPM. CYCLIC STRESS TEST UNITS

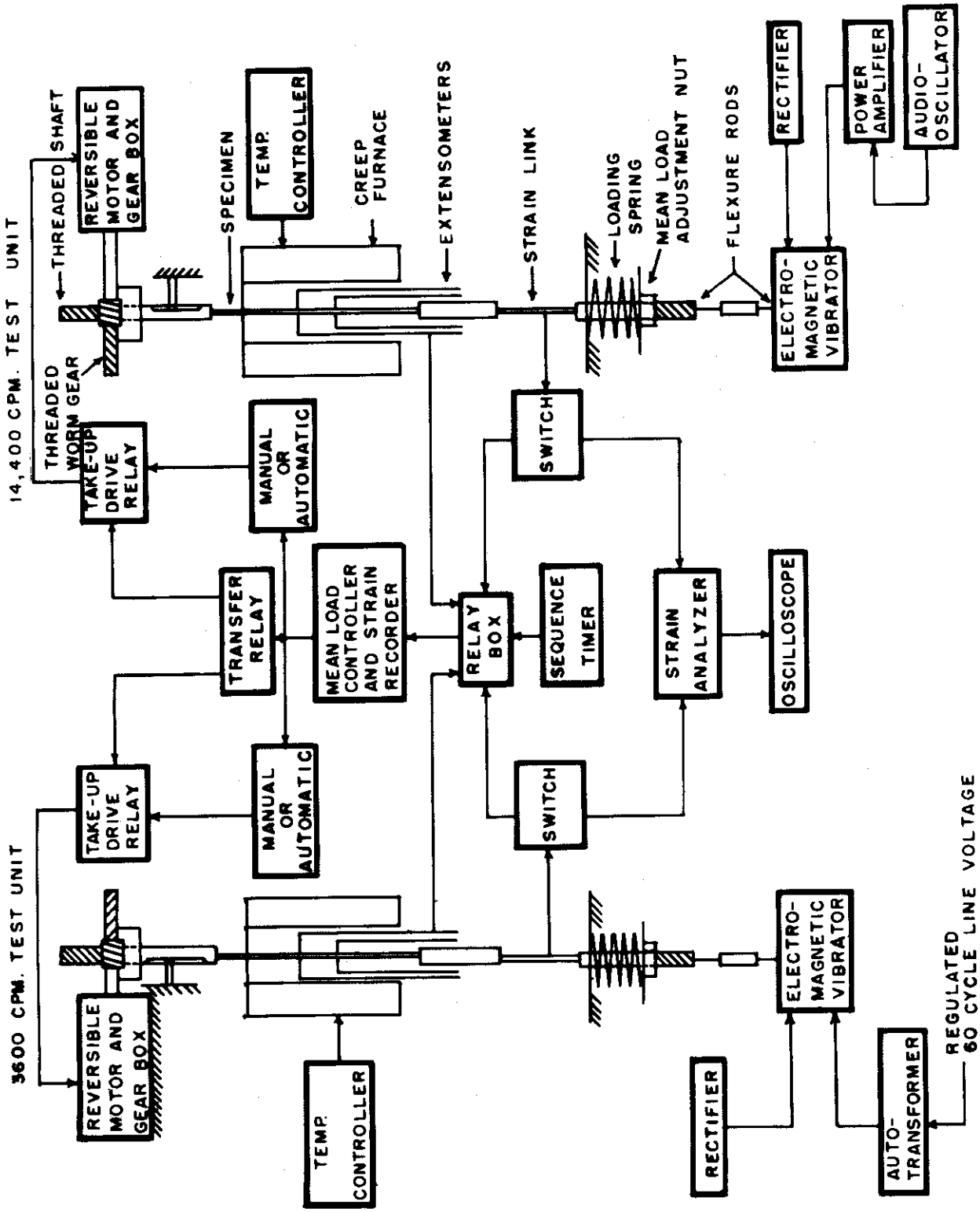

FIGURE 3 SCHEMATIC DIAGRAM OF 3600 AND 14,400 CPM. CYCLIC TEST UNITS

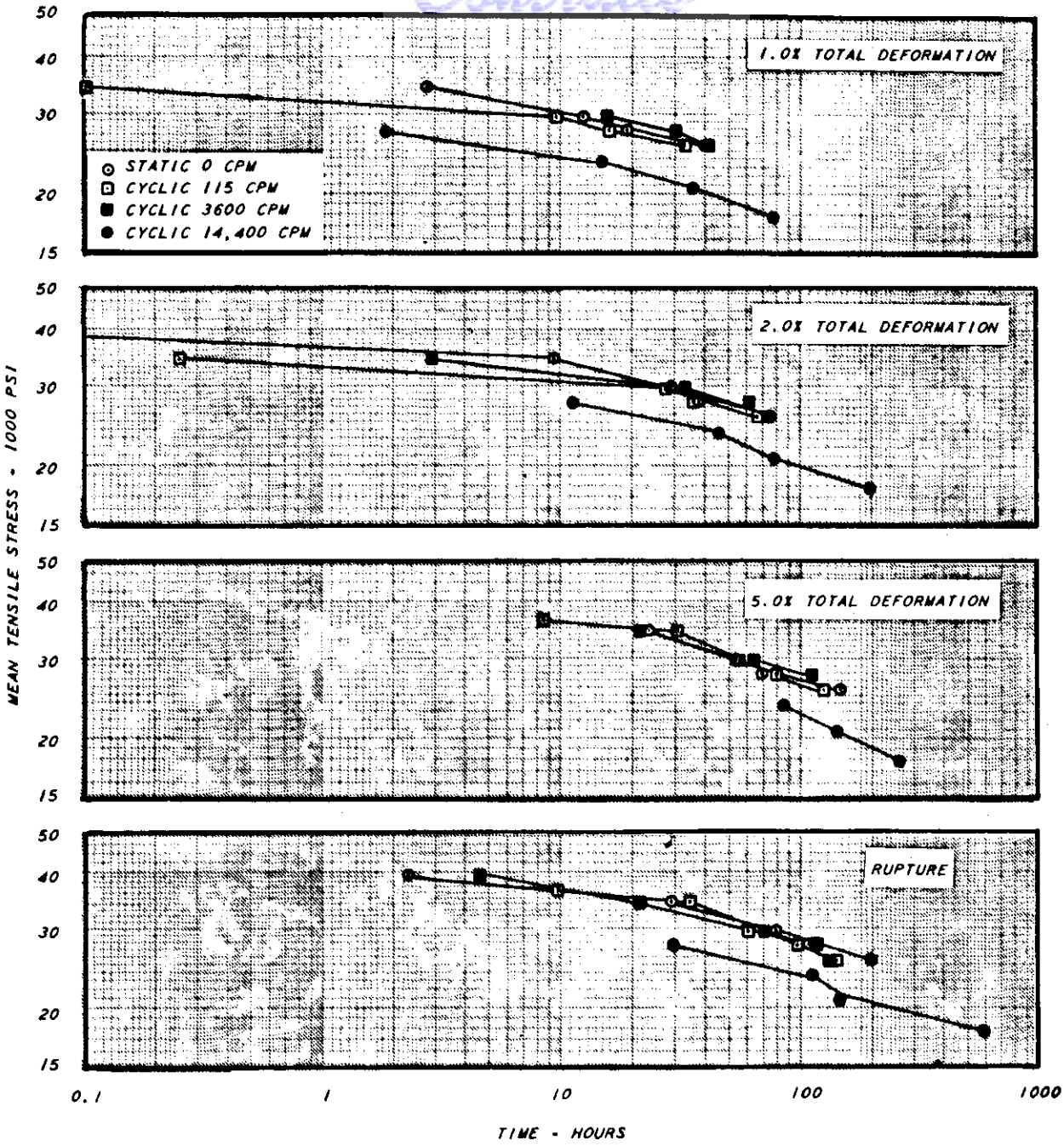

Figure 4 STRESS-TIME RELATIONSHIPS OF ANNEALED LOW CARBON N-155 SHEET DYNAMICALLY STRESSED AT 1350°F FOR STRESS AMPLITUDES OF 0 AND 25% AT VARIOUS STRESSING FREQUENCIES.

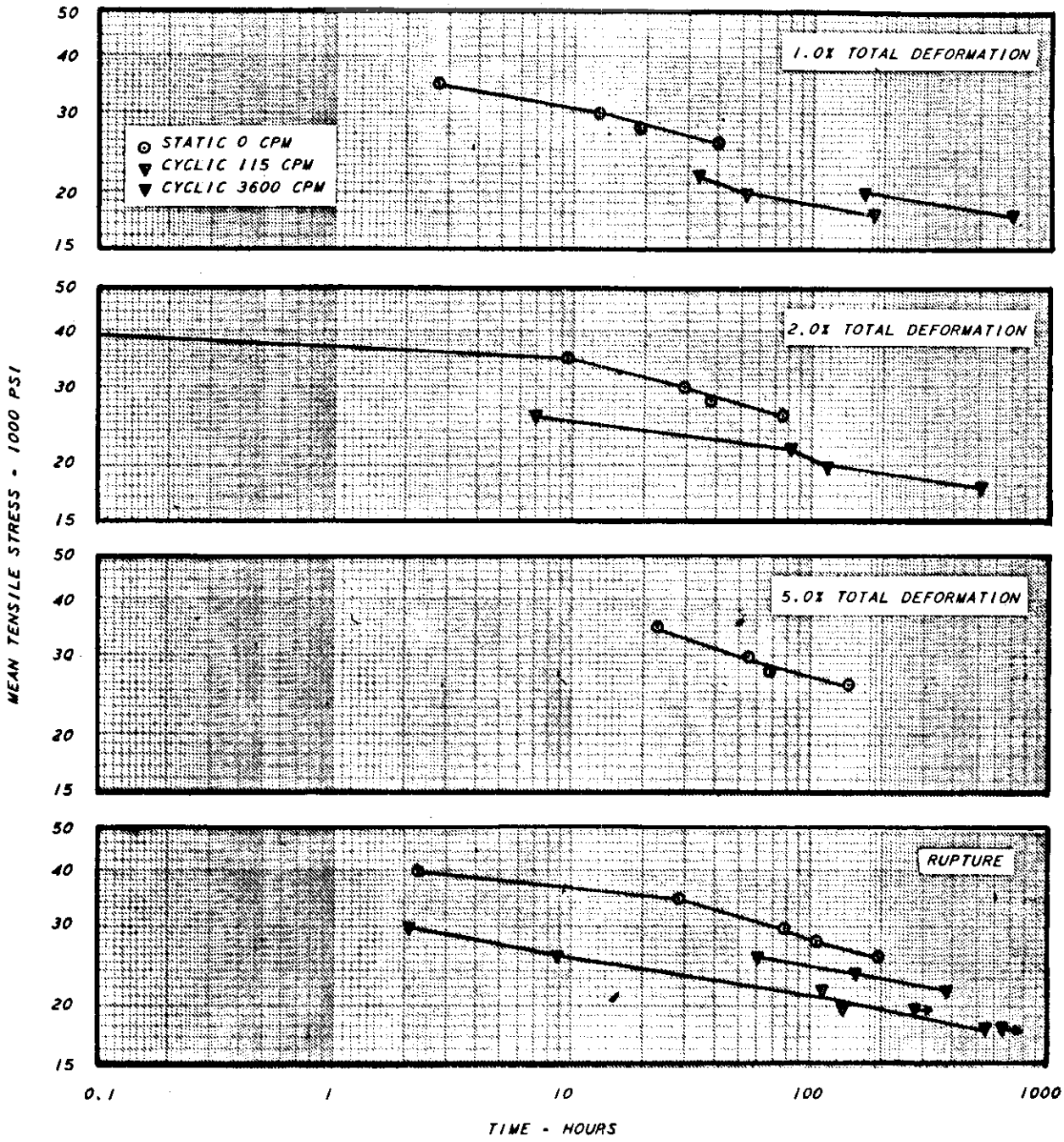

Figure 5 STRESS-TIME RELATIONSHIPS OF ANNEALED LOW CARBON N-155 SHEET DYNAMICALLY STRESSED AT 1350°F FOR STRESS AMPLITUDES OF 0 AND 67% AT VARIOUS STRESSING FREQUENCIES.

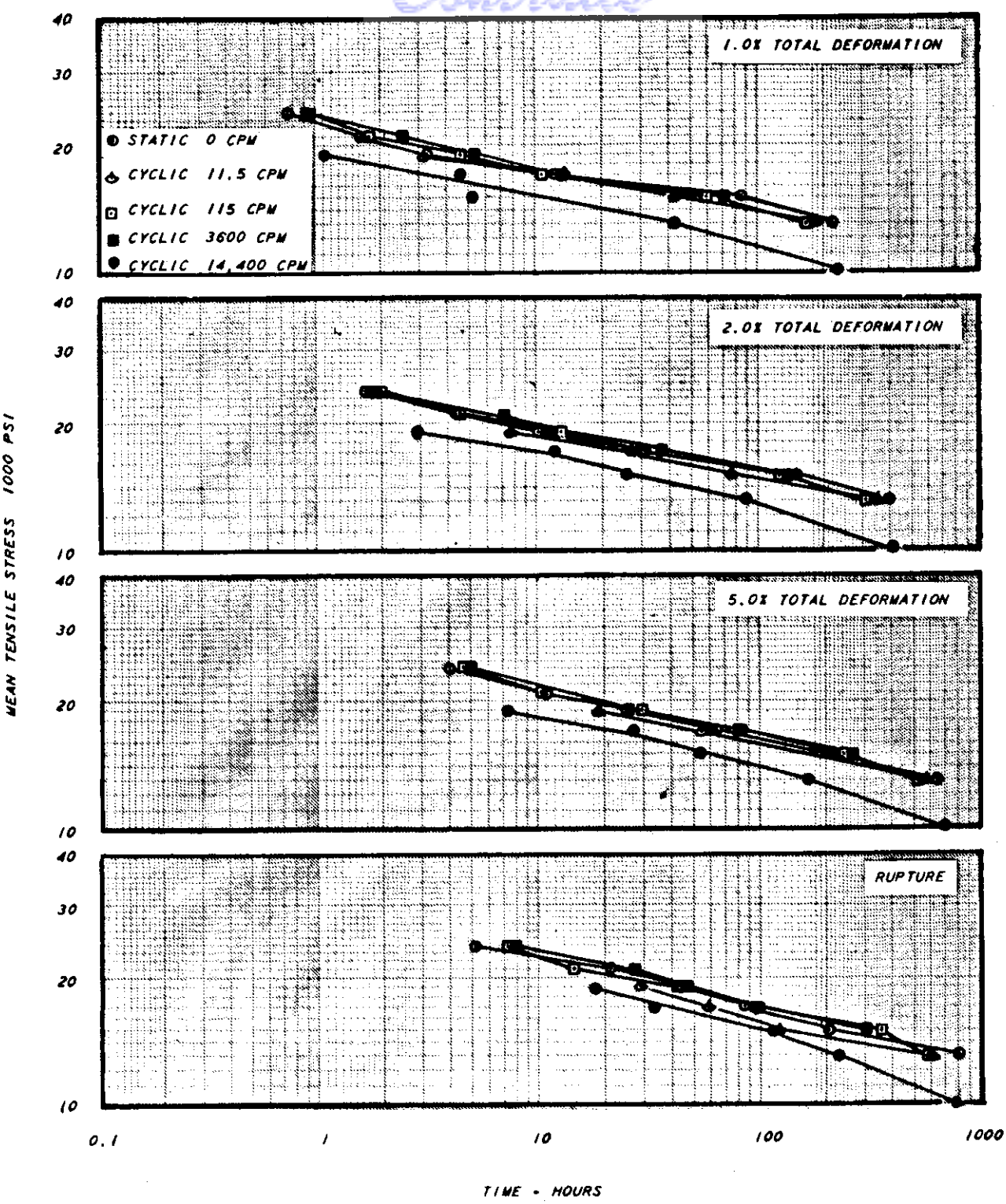

Figure 6 STRESS-TIME RELATIONSHIPS OF ANNEALED LOW CARBON N-155 SHEET DYNAMICALLY STRESSED AT 1500°F FOR STRESS AMPLITUDES OF 0 AND 25% AT VARIOUS STRESSING FREQUENCIES

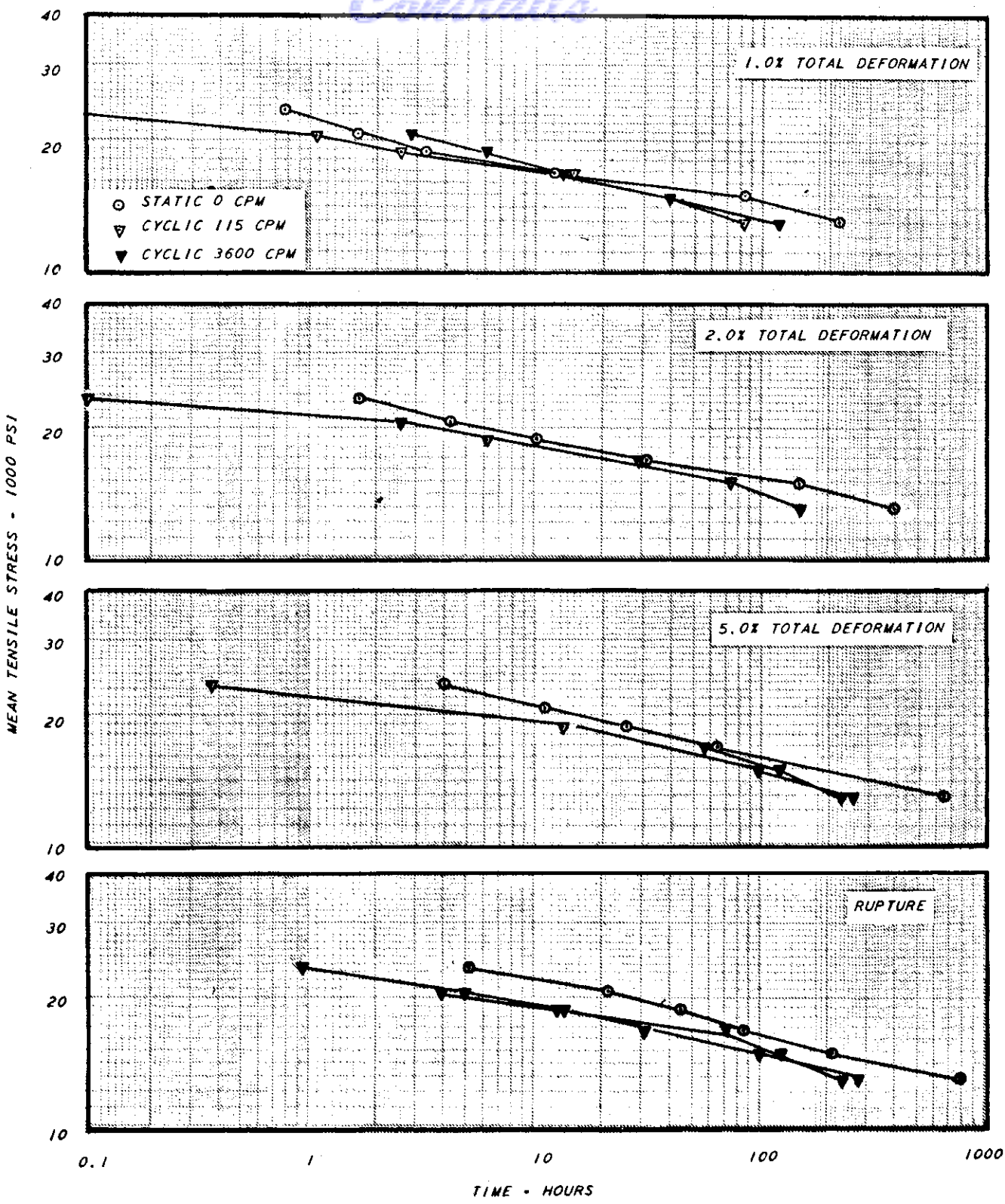

Figure 7 STRESS-TIME RELATIONSHIPS OF ANNEALED LOW CARBON N-155 SHEET DYNAMICALLY STRESSED AT 1500°F FOR STRESS AMPLITUDES OF 0 AND 67% AT VARIOUS STRESSING FREQUENCIES.

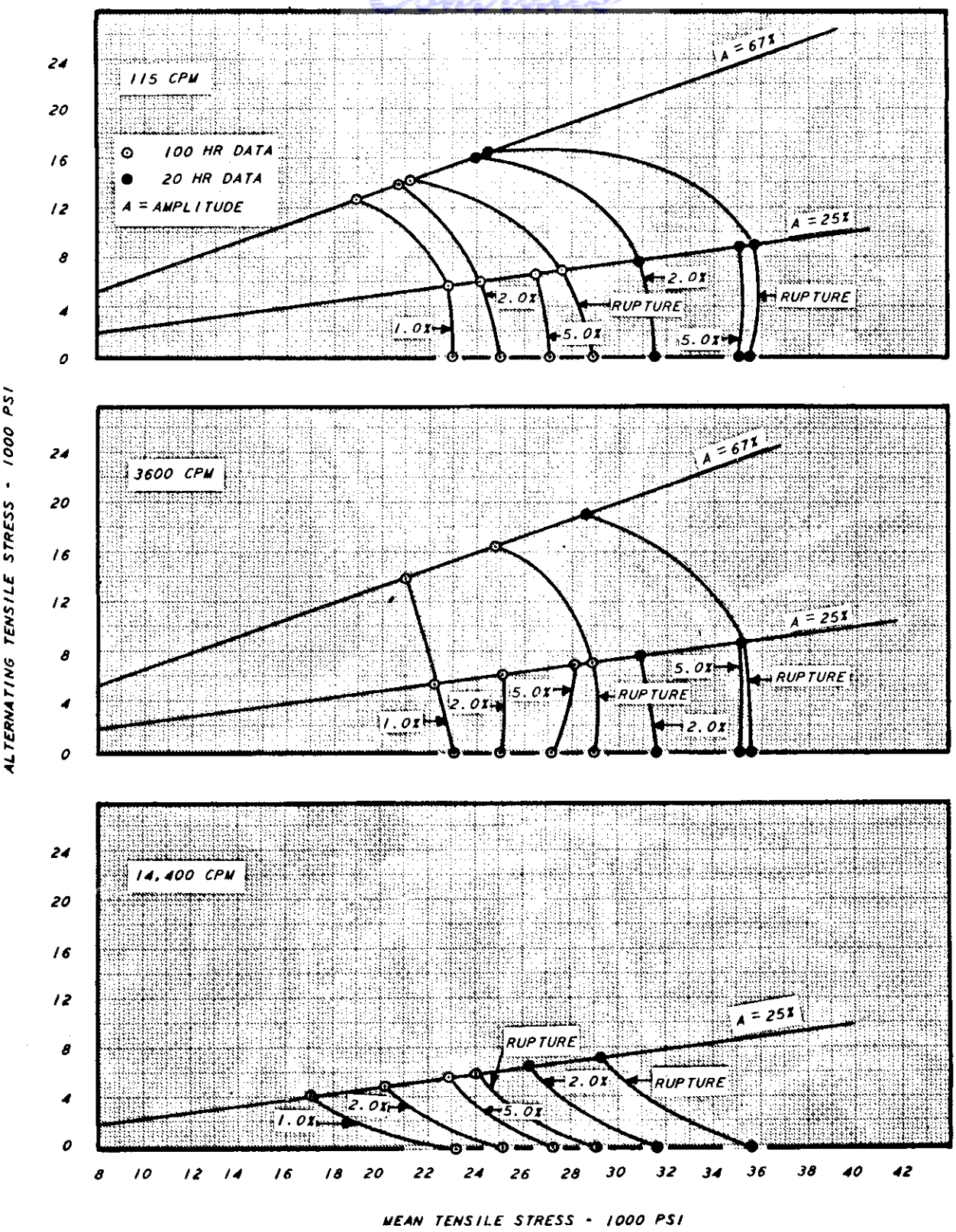

Figure 8 STRESS COMBINATIONS AT VARIOUS FREQUENCIES FOR TOTAL DEFORMATION AND RUPTURE OF ANNEALED LOW CARBON N-155 SHEET AT 1350°F

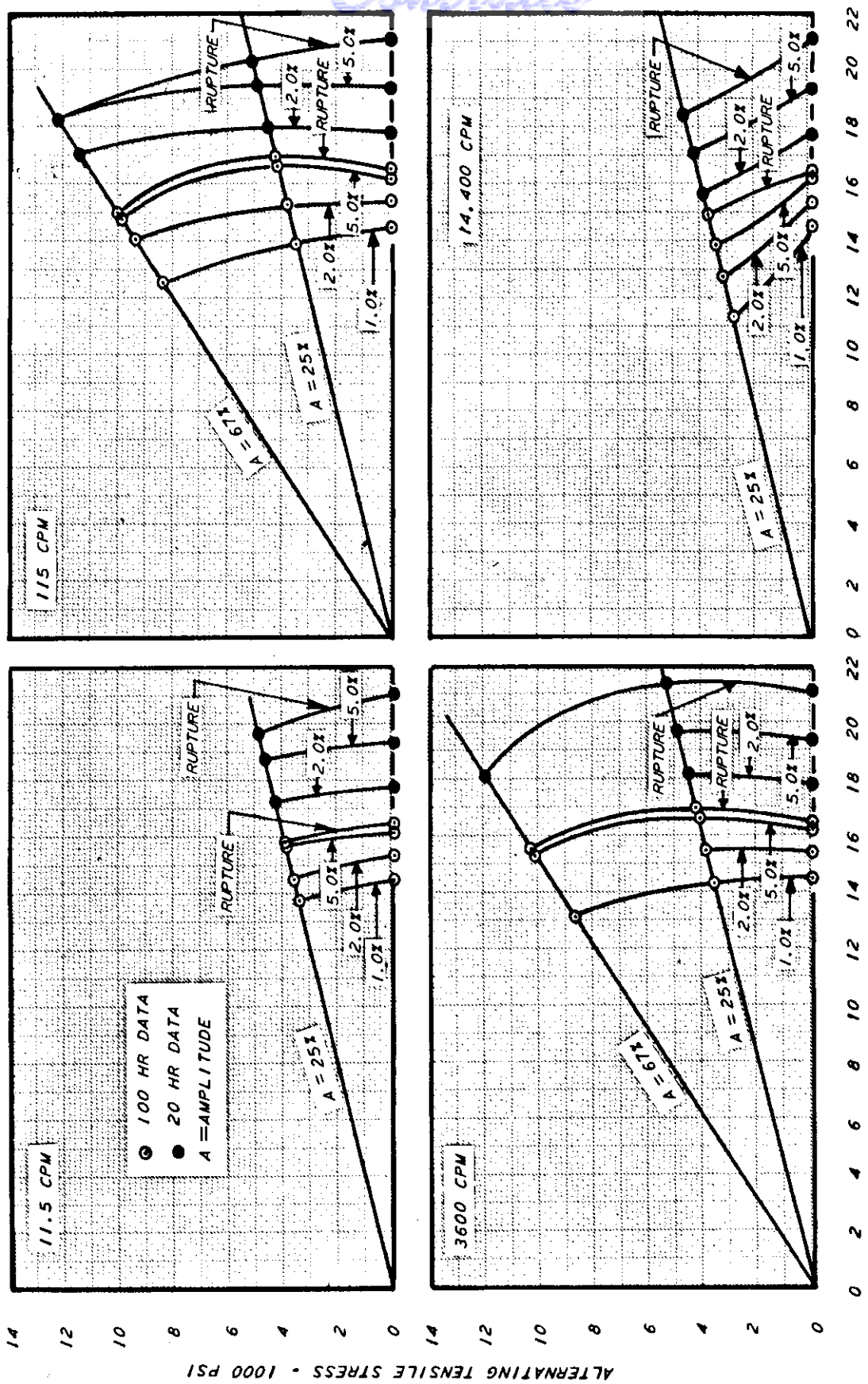

Figure 9 STRESS COMBINATIONS AT VARIOUS FREQUENCIES FOR TOTAL DEFORMATION AND RUPTURE OF ANNEALED LOW CARBON N-155 SHEET AT 1500°F

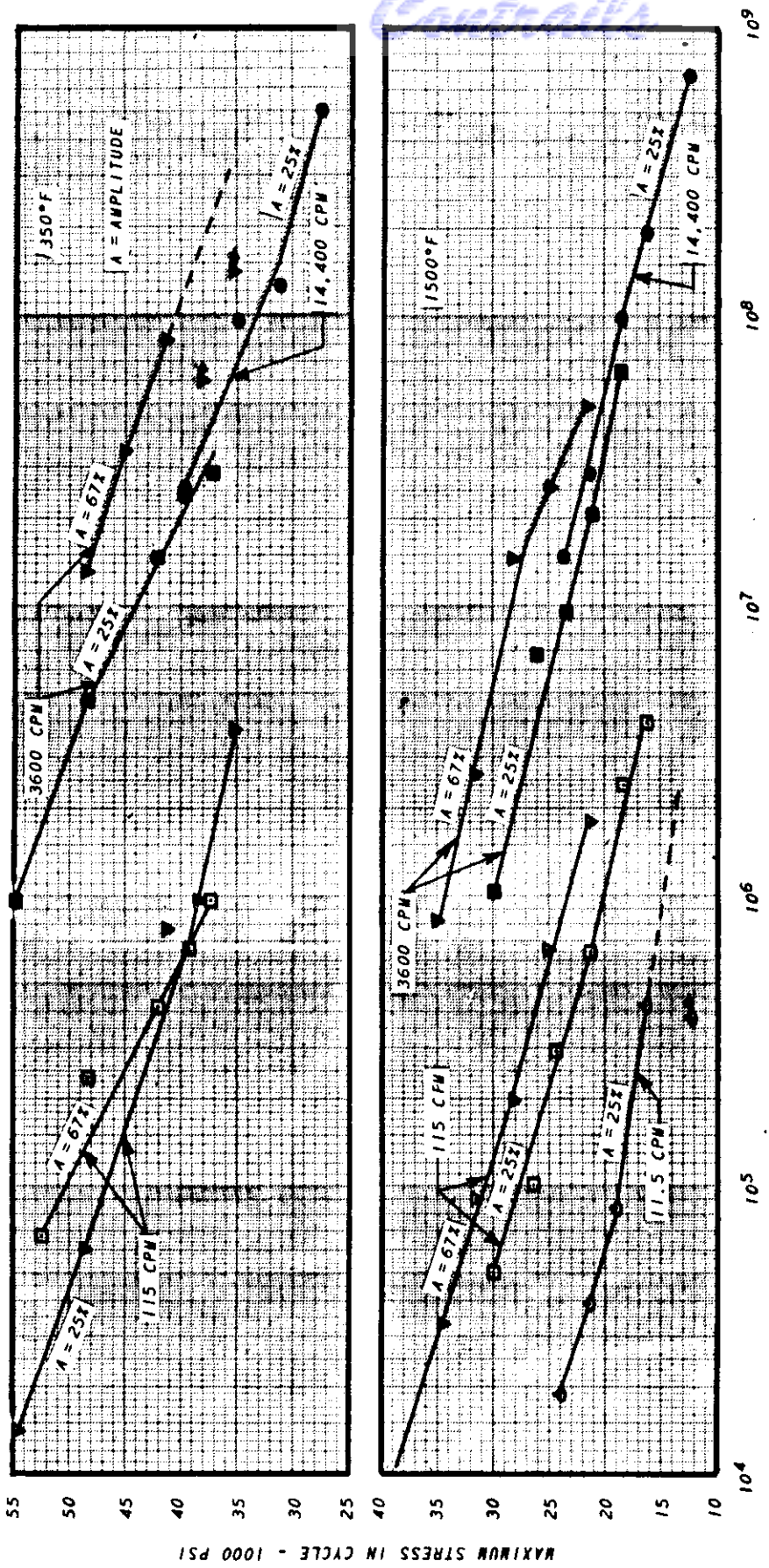

Figure 10 MAXIMUM STRESS Vs. NUMBER OF CYCLES TO RUPTURE FOR ANNEALED LOW CARBON N-155 SHEET UNDER VARIOUS DIRECT STRESSING CONDITIONS AT 1350 AND 1500°F

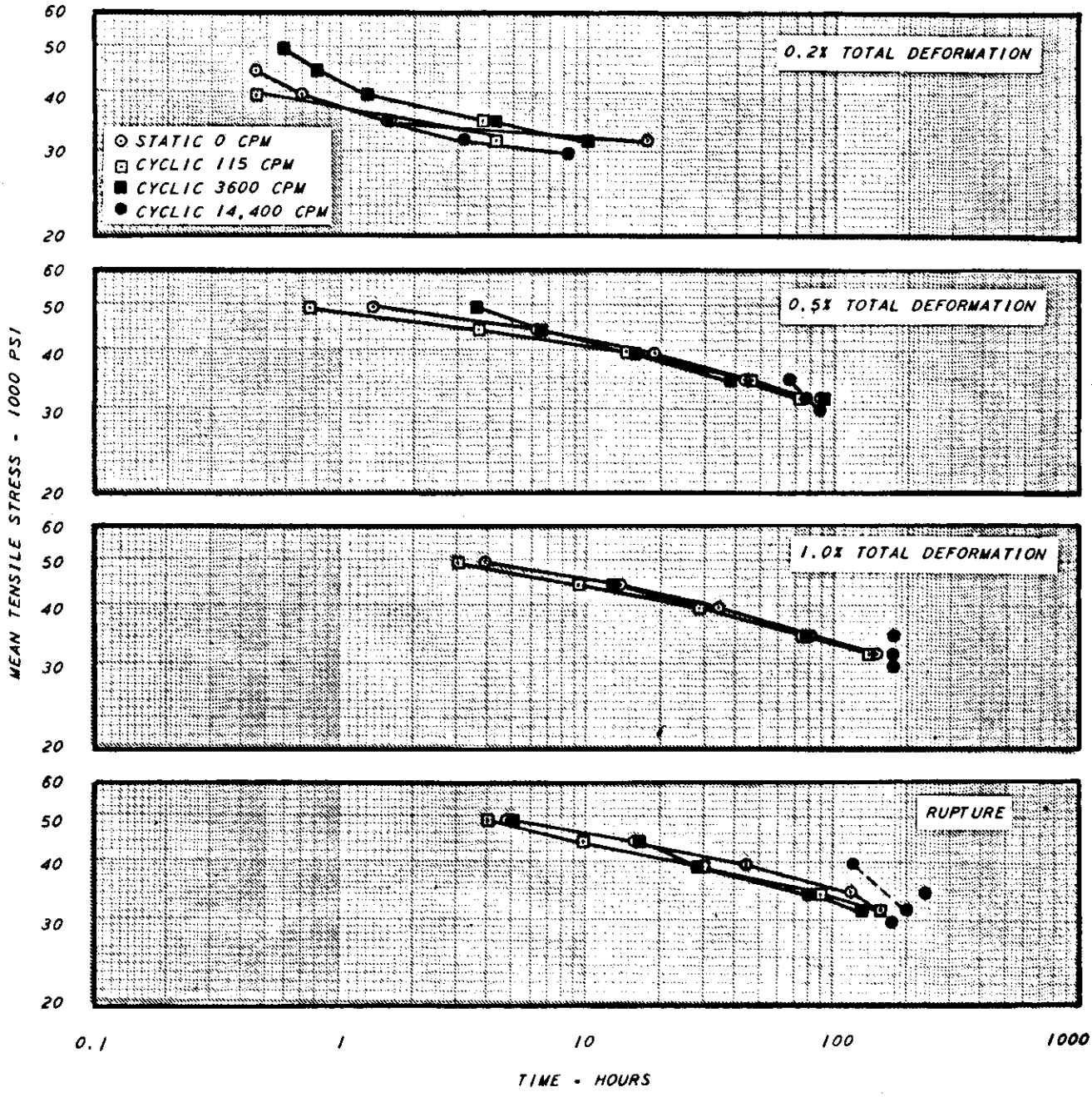

Figure 11 STRESS-TIME RELATIONSHIPS OF AGED INCONEL X SHEET DYNAMICALLY STRESSED AT 1350° F FOR STRESS AMPLITUDES OF 0 AND 25% AT VARIOUS STRESSING FREQUENCIES.

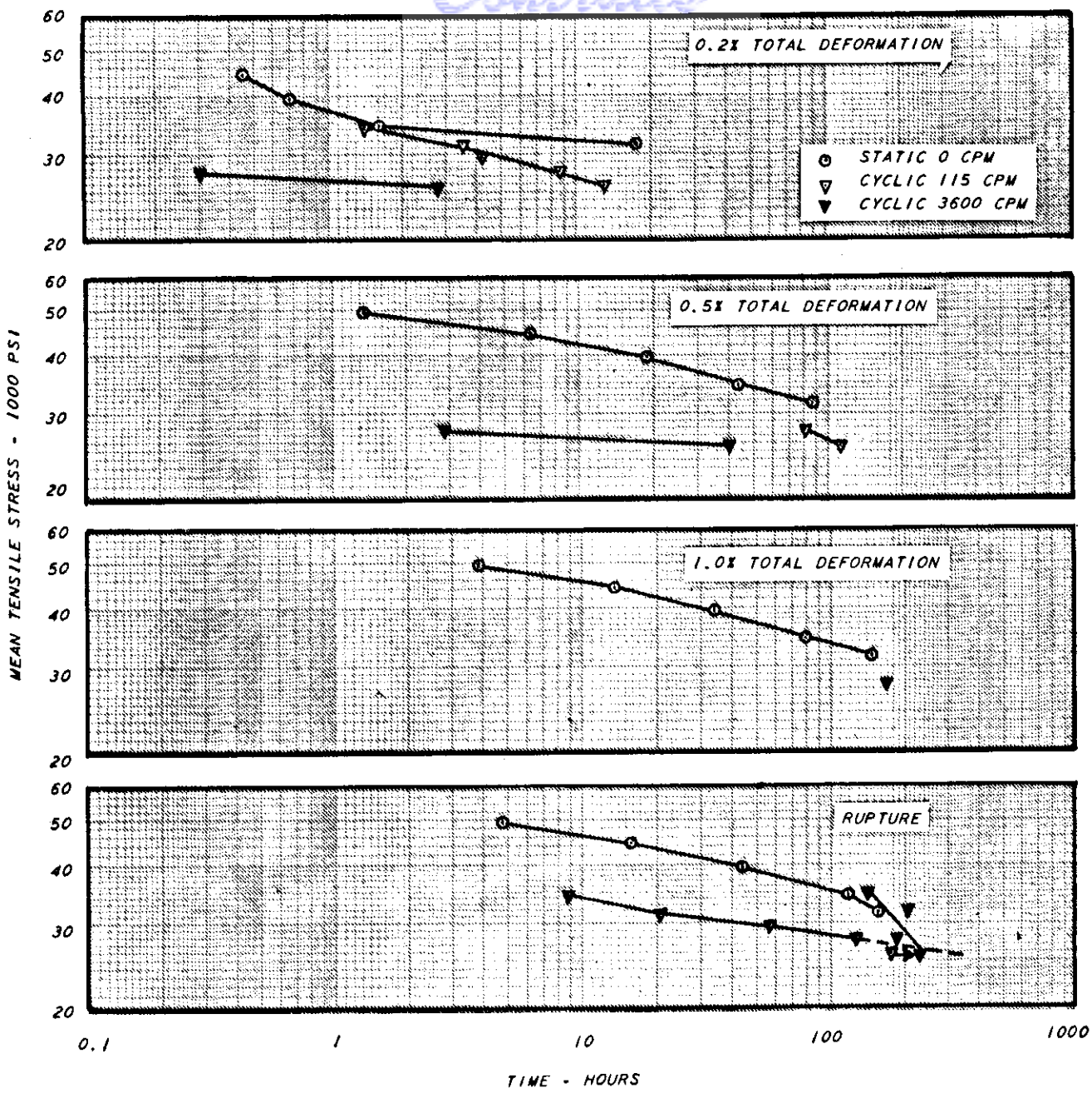

Figure 12 STRESS-TIME RELATIONS OF AGED INCONEL X SHEET DYNAMICALLY STRESSED AT 1350°F FOR STRESS AMPLITUDES OF 0 AND 67% AT VARIOUS STRESSING FREQUENCIES

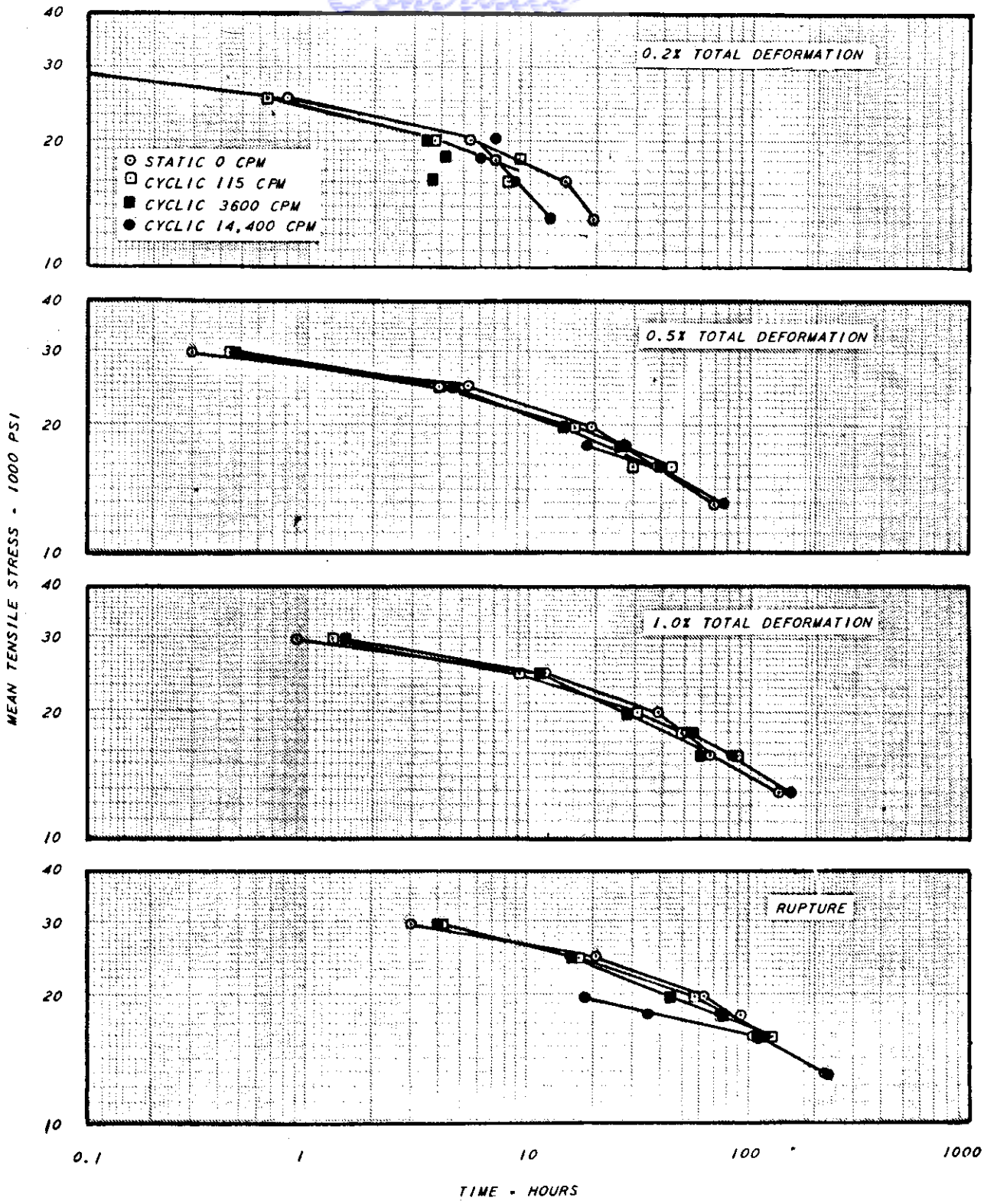

Figure 13 STRESS-TIME RELATIONSHIPS OF AGED INCONEL X SHEET DYNAMICALLY STRESSED AT 1500°F FOR STRESS AMPLITUDES OF 0 AND 25% AT VARIOUS FREQUENCIES.

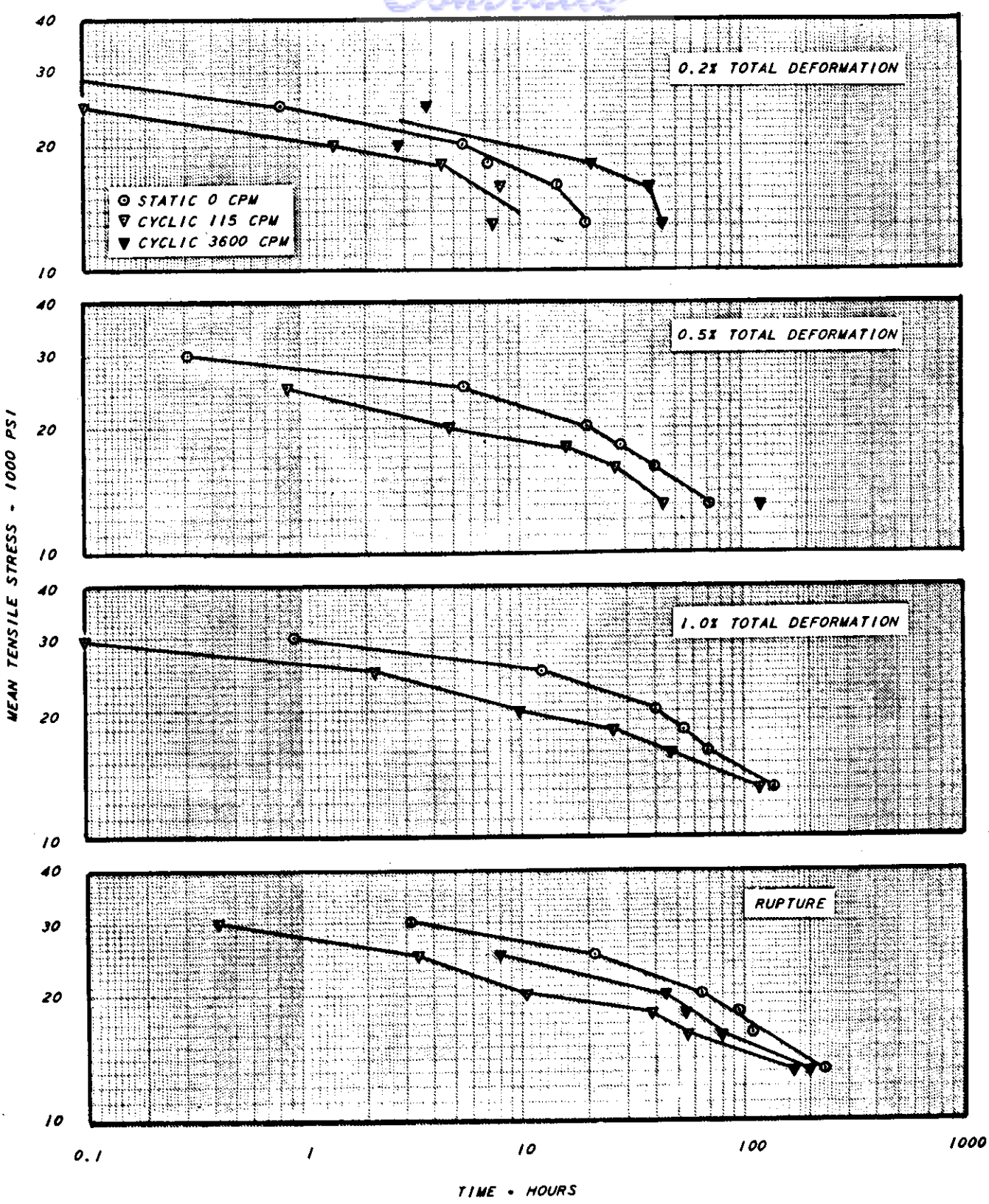

Figure 14 STRESS-TIME RELATIONSHIPS OF AGED INCONEL X SHEET DYNAMICALLY STRESSED AT 1500°F FOR STRESS AMPLITUDES OF 0 AND 67% AT VARIOUS FREQUENCIES

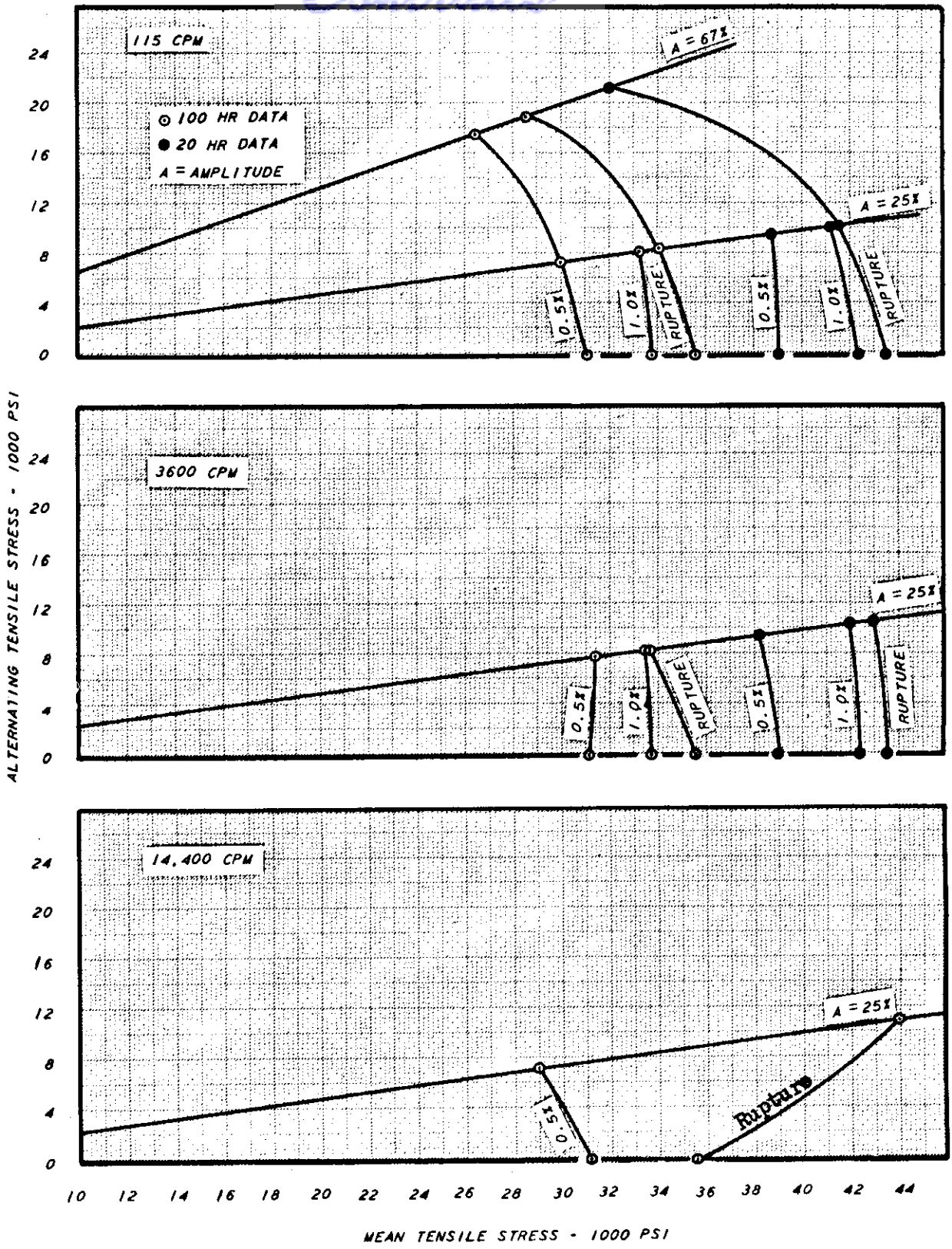

Figure 15 STRESS COMBINATIONS AT VARIOUS FREQUENCIES FOR TOTAL DEFORMATION AND RUPTURE OF AGED INCONEL X SHEET AT 1350°F

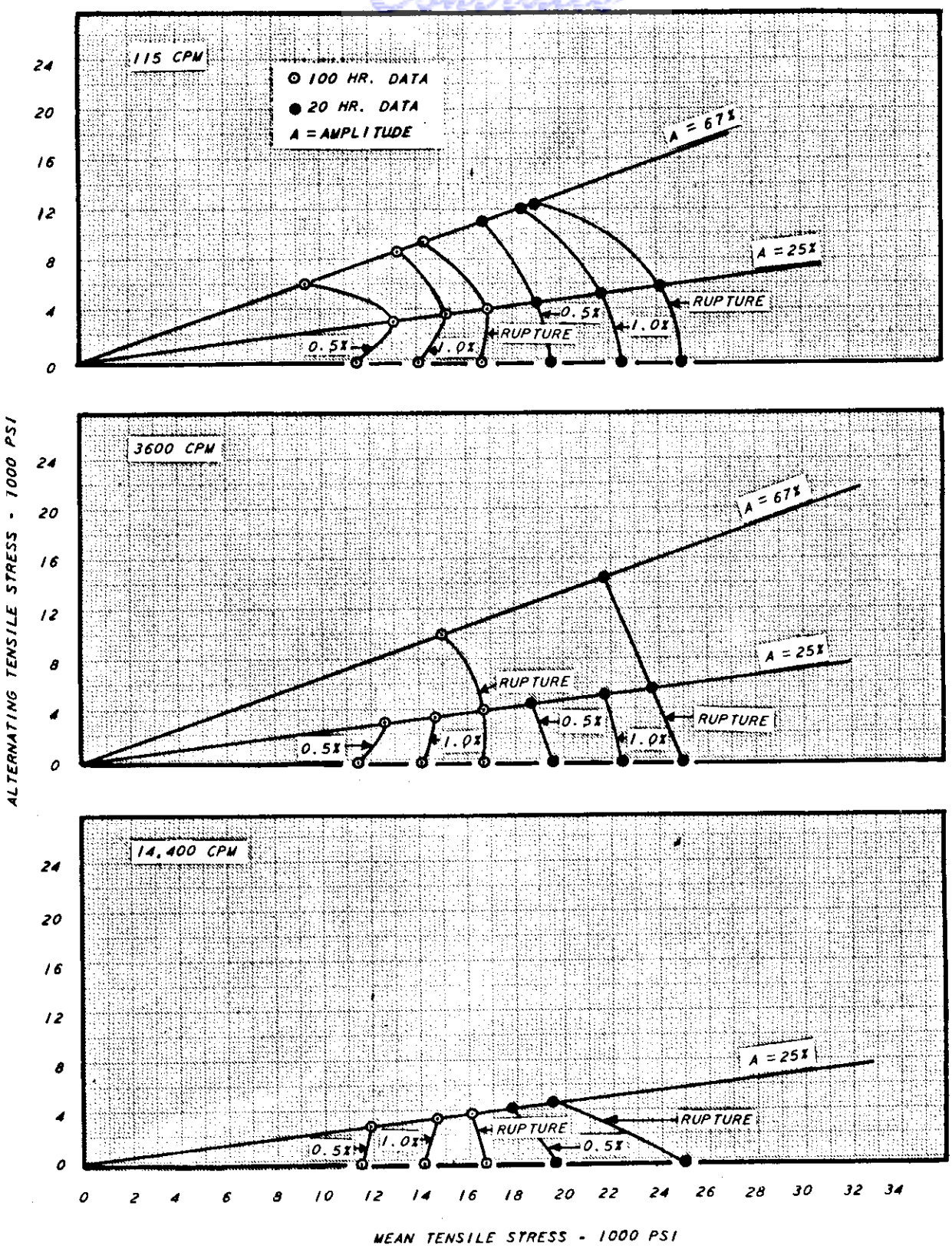

Figure 16 STRESS COMBINATIONS AT VARIOUS FREQUENCIES FOR TOTAL DEFORMATION AND RUPTURE OF AGED INCONEL X SHEET AT 1500°F

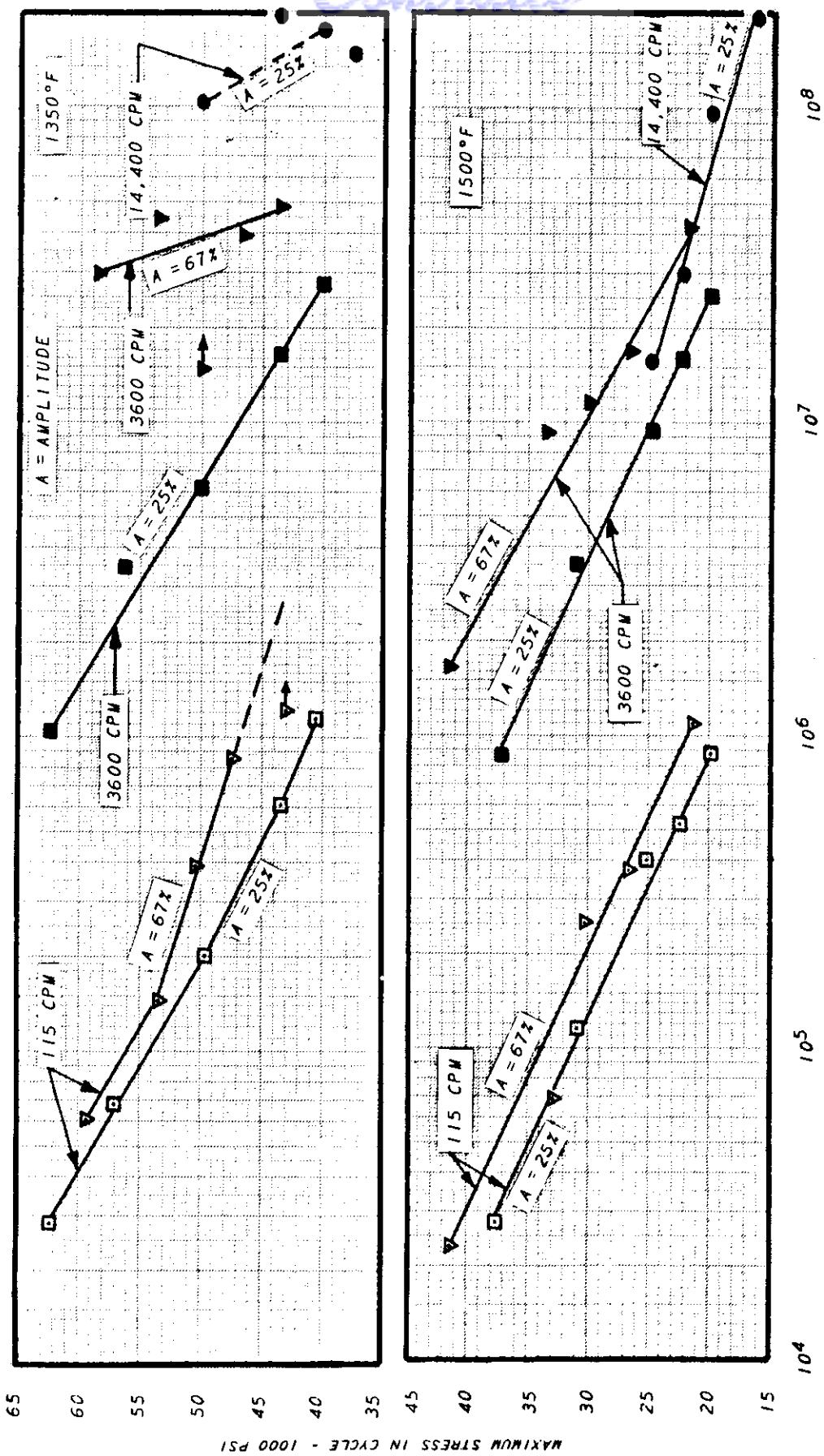

Figure 17 MAXIMUM STRESS Vs. NUMBER OF CYCLES TO RUPTURE FOR AGED INCONEL X SHEET UNDER VARIOUS DIRECT STRESSING CONDITIONS AT 1350 AND 1500°F

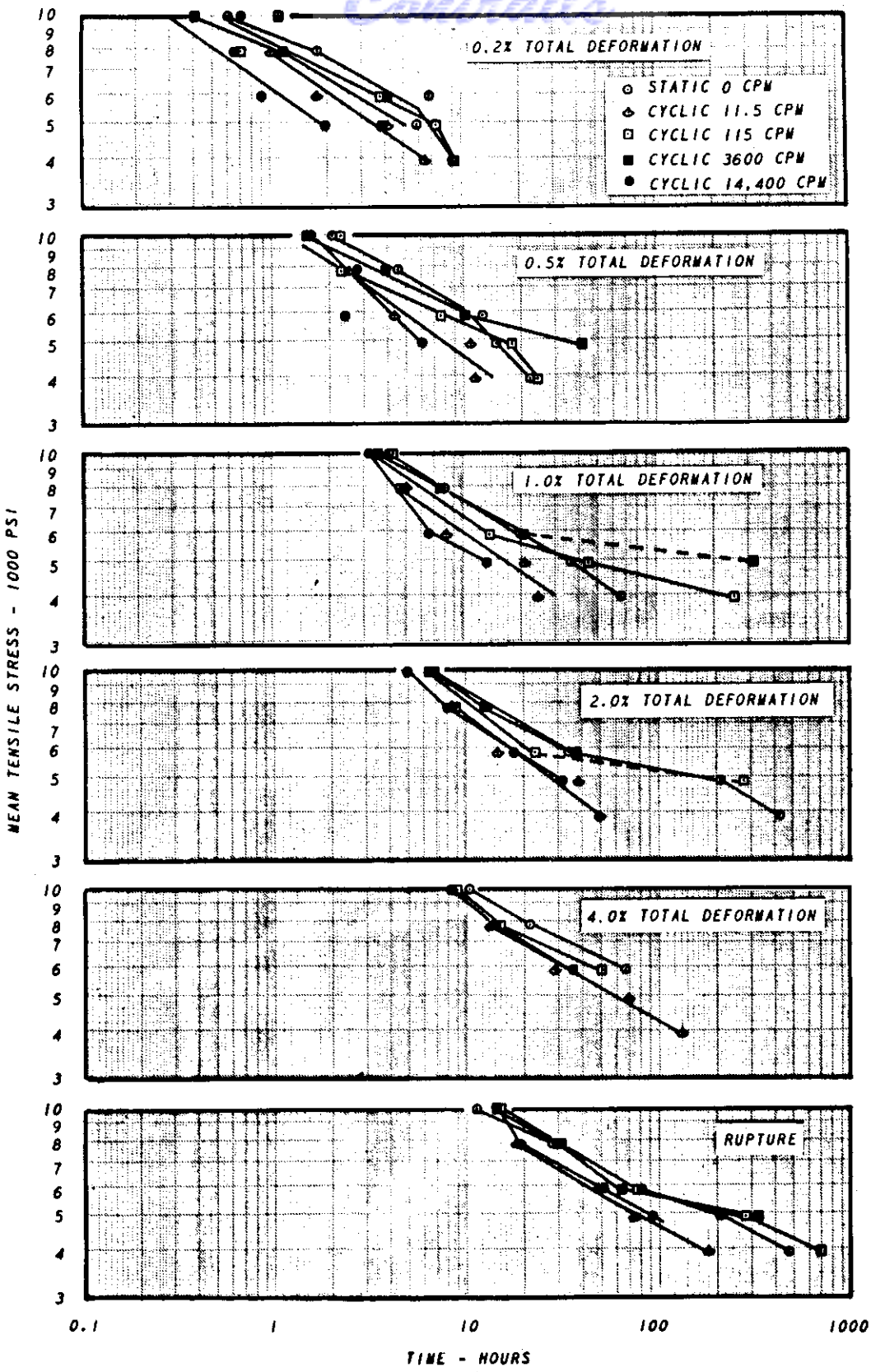

Figure 18 STRESS-TIME RELATIONSHIPS OF TYPE 321 STAINLESS STEEL SHEET DYNAMICALLY STRESSED AT 1500°F FOR STRESS AMPLITUDES OF 0 AND 25% AT VARIOUS STRESSING FREQUENCIES

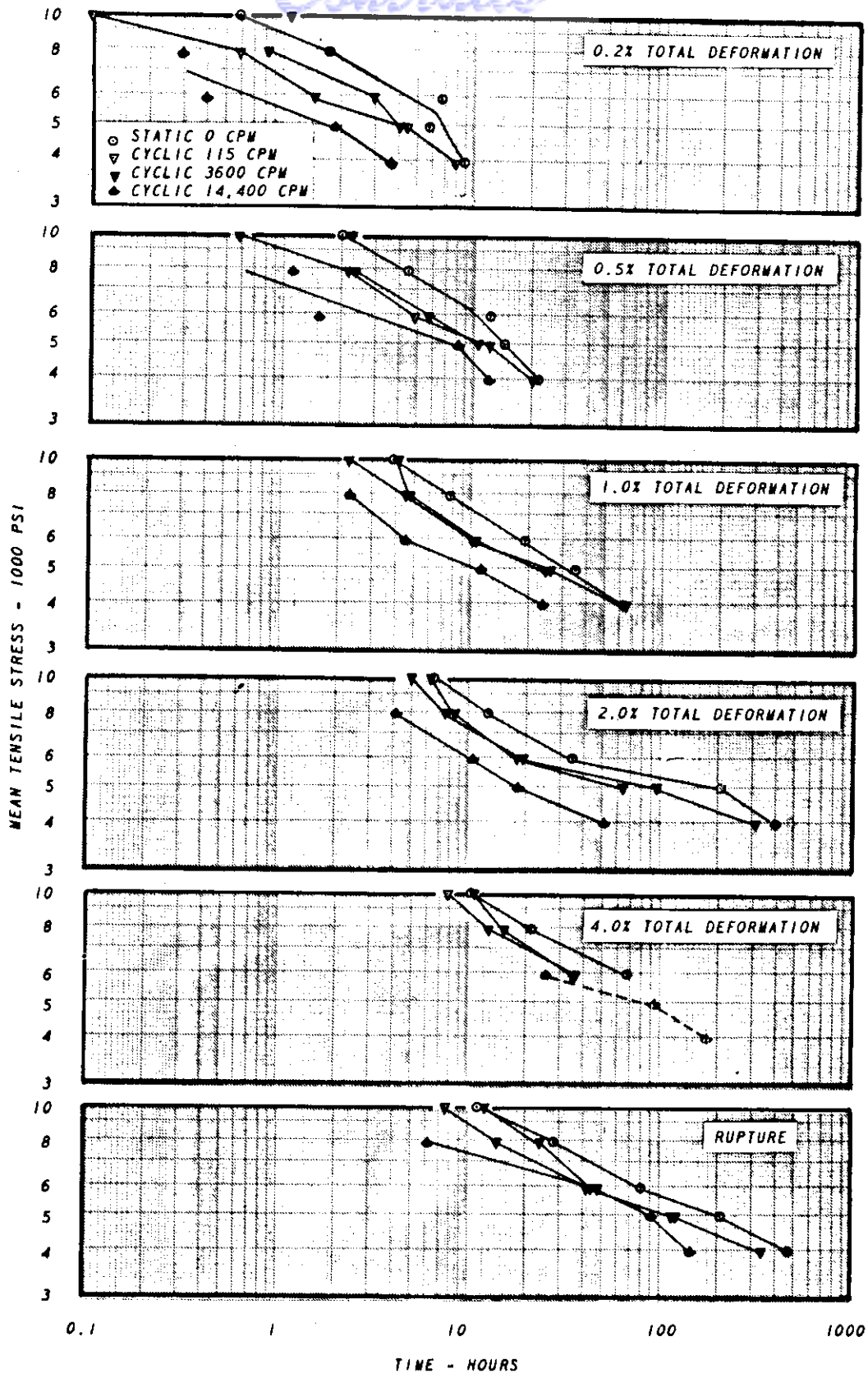

Figure 19 STRESS-TIME RELATIONSHIPS OF TYPE 321 STAINLESS STEEL SHEET DYNAMICALLY STRESSED AT 1500°F FOR STRESS AMPLITUDES OF 0 AND 67% AT VARIOUS STRESSING FREQUENCIES.

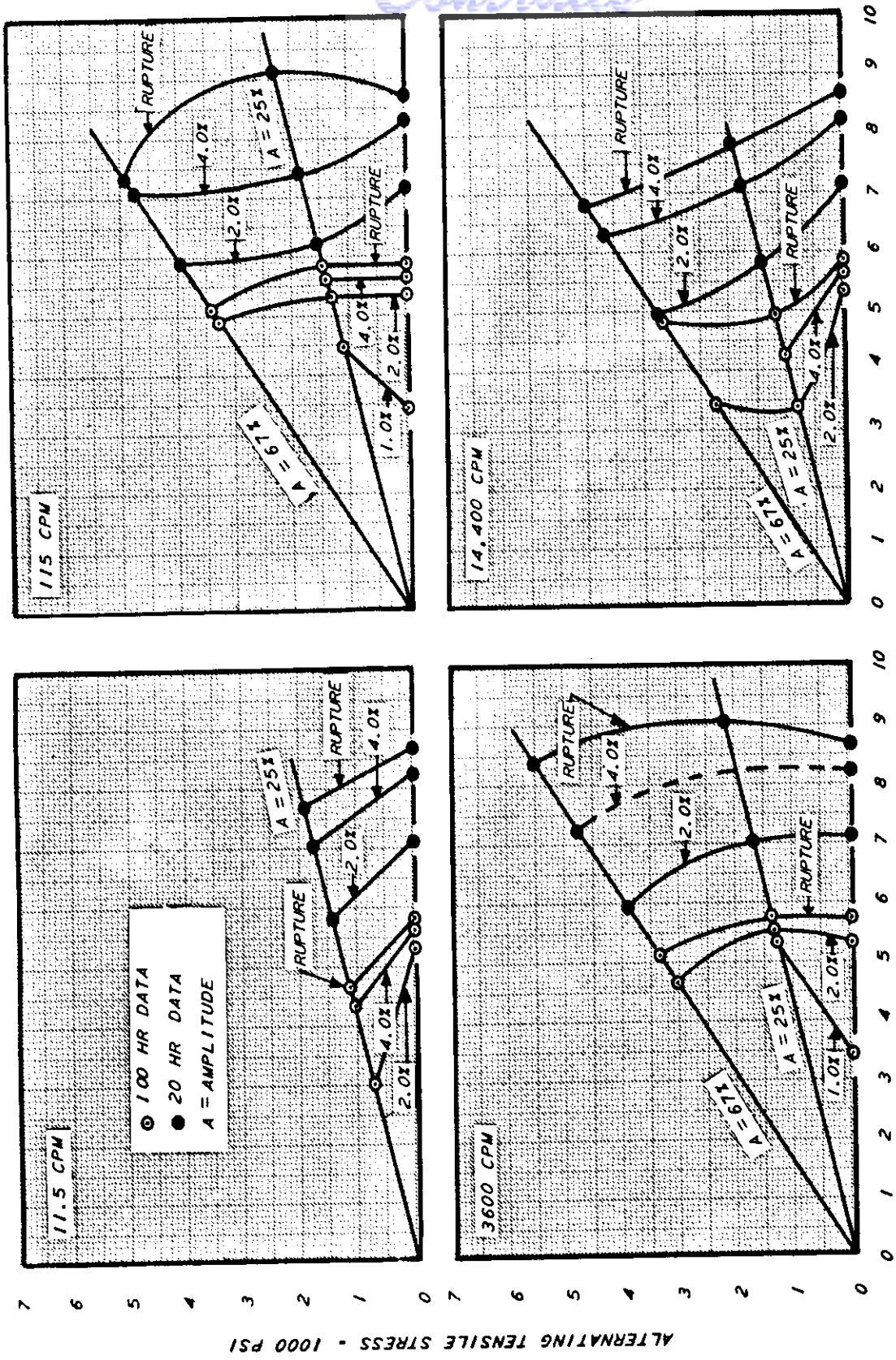

Figure 20 STRESS COMBINATIONS AT VARIOUS FREQUENCIES FOR TOTAL DEFORMATION AND RUPTURE OF TYPE 321 STAINLESS STEEL SHEET AT 1500°F

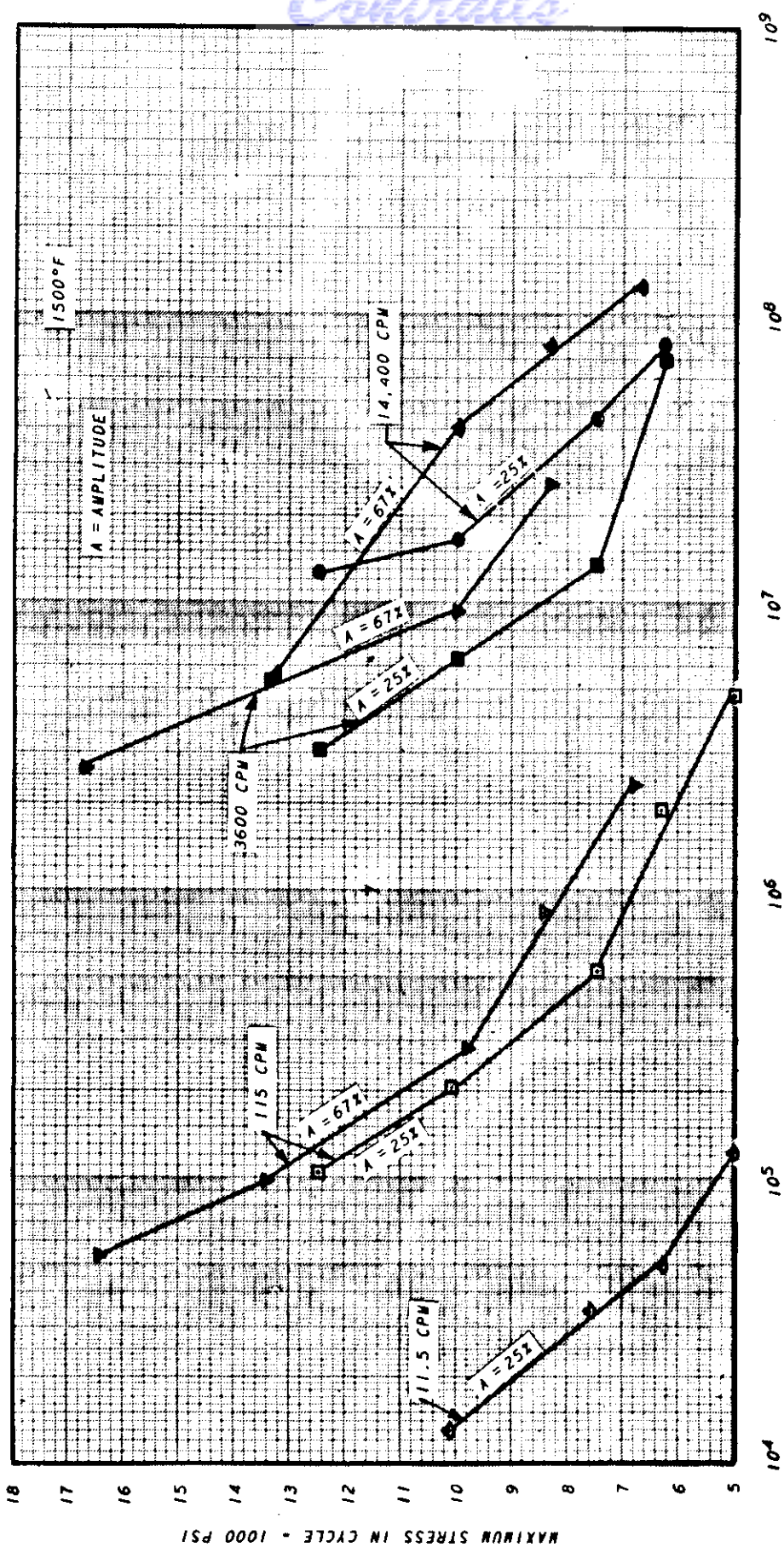

Figure 21 MAXIMUM STRESS Vs. NUMBER OF CYCLES TO RUPTURE FOR TYPE 321 STAINLESS STEEL SHEET UNDER VARIOUS DIRECT STRESSING CONDITIONS AT 1500°F

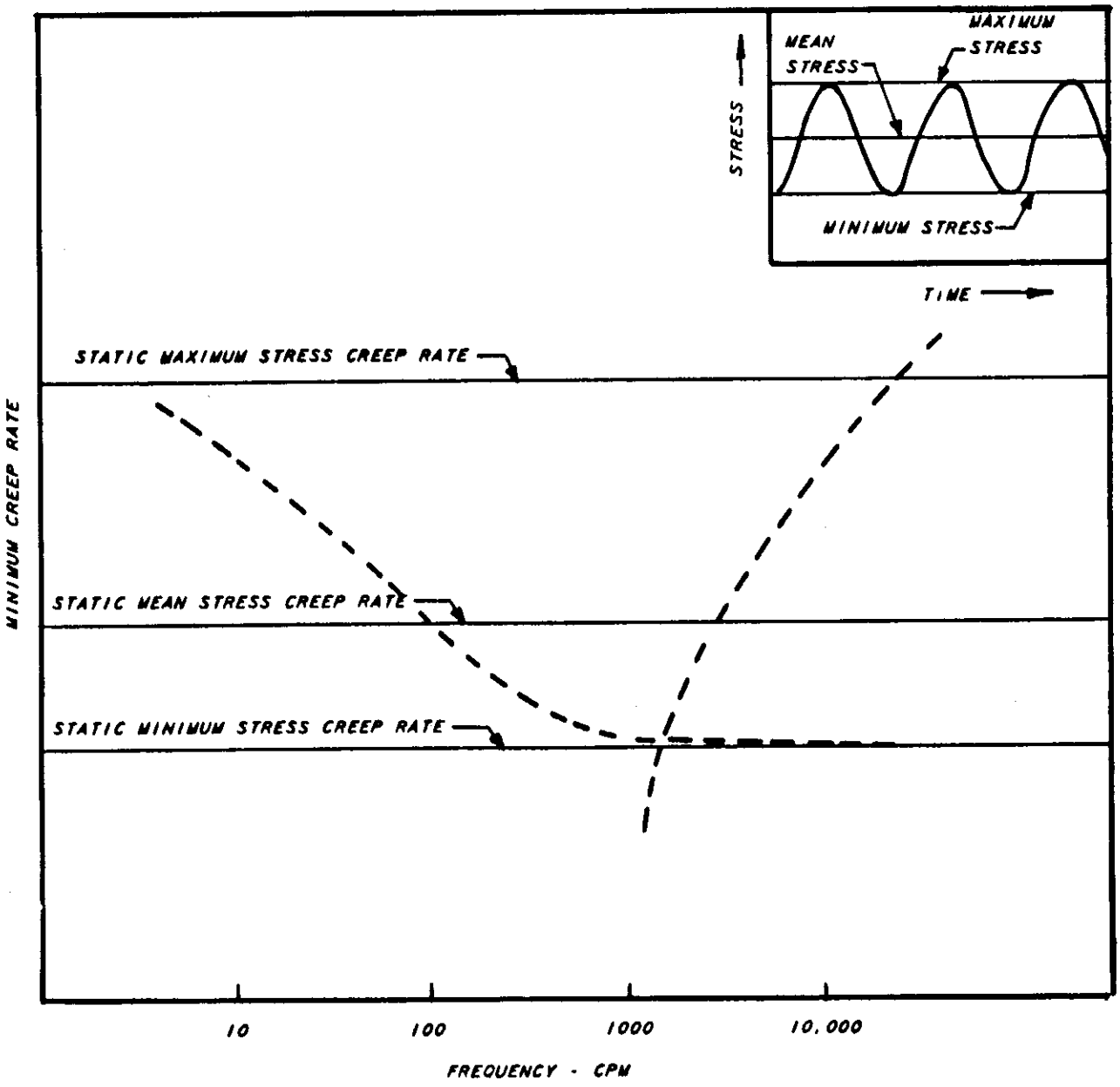

Figure 22 SCHEMATIC REPRESENTATION OF CREEP RATE Vs. FREQUENCY OF AN ALLOY AT CONSTANT TEMPERATURE, CONSTANT MEAN STRESS, AND CONSTANT AMPLITUDE

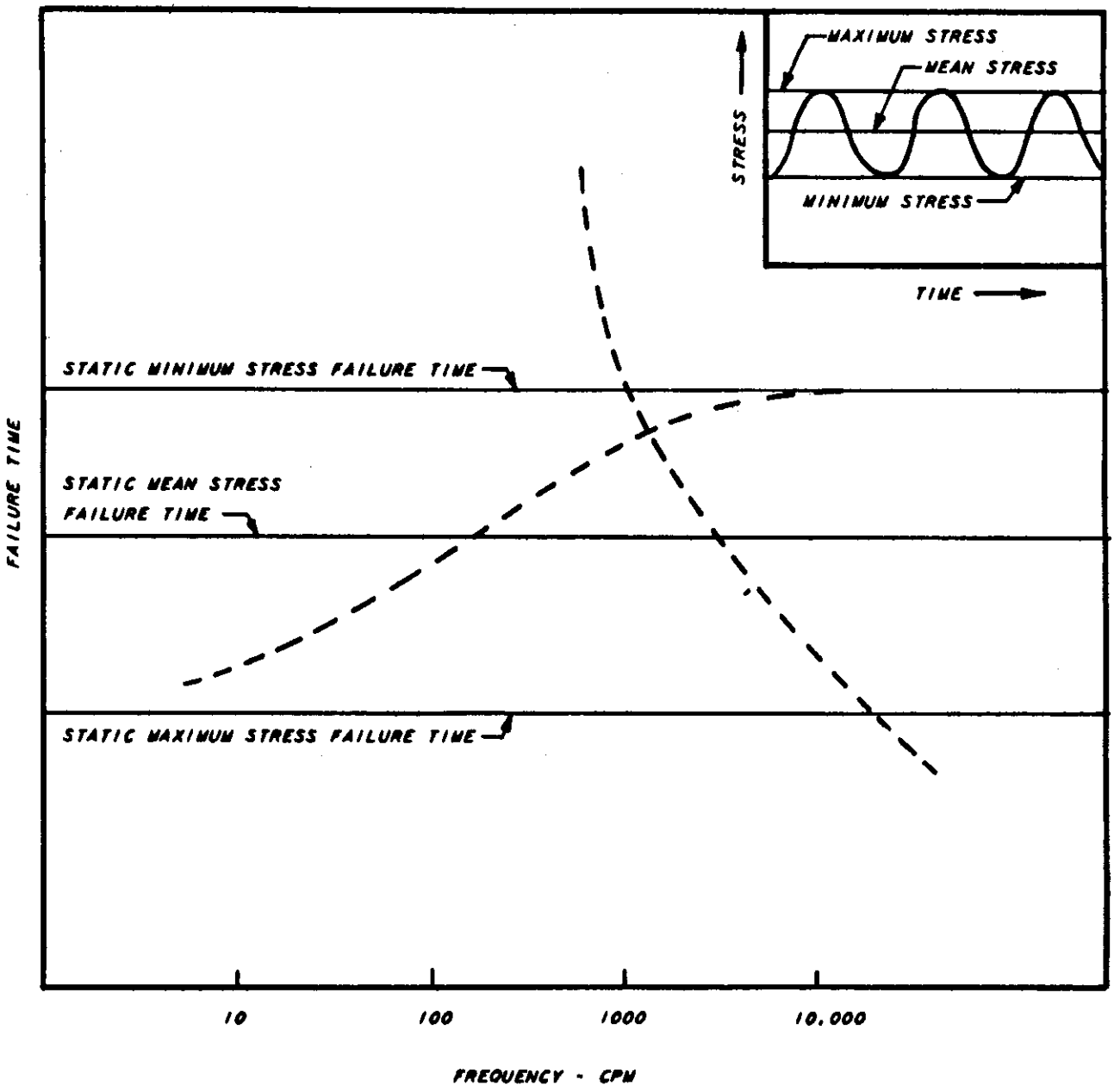

Figure 23 SCHEMATIC REPRESENTATION OF FAILURE TIME Vs. FREQUENCY OF AN ALLOY AT CONSTANT TEMPERATURE, CONSTANT MEAN STRESS, AND CONSTANT AMPLITUDE

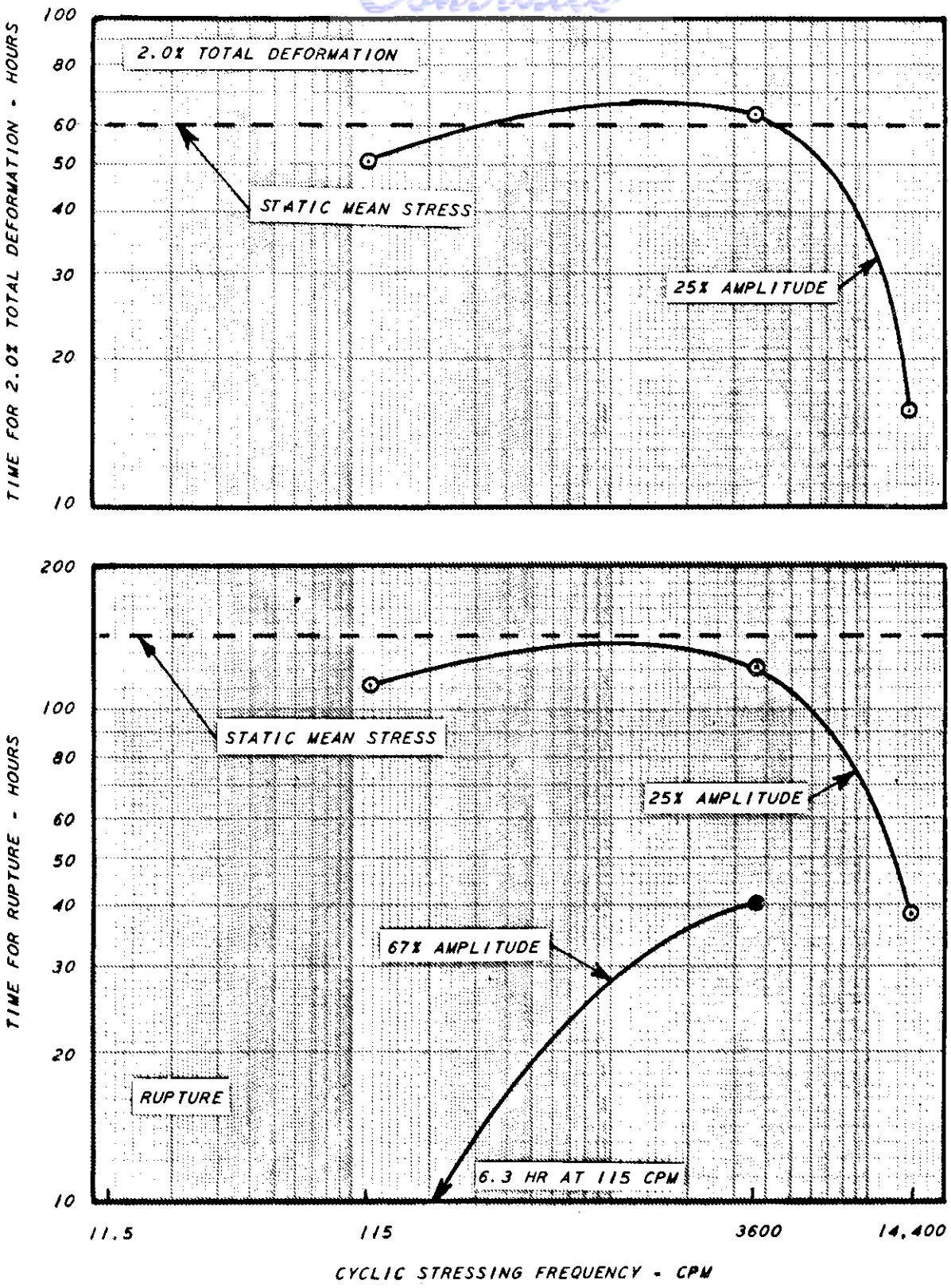

Figure 24 EFFECT OF CYCLIC STRESSING FREQUENCY AND AMPLITUDE ON THE DEFORMATION AND RUPTURE CHARACTERISTICS OF ANNEALED LOW CARBON N-155 SHEET AT 1350°F FOR A CONSTANT MEAN STRESS OF 27,000 PSI

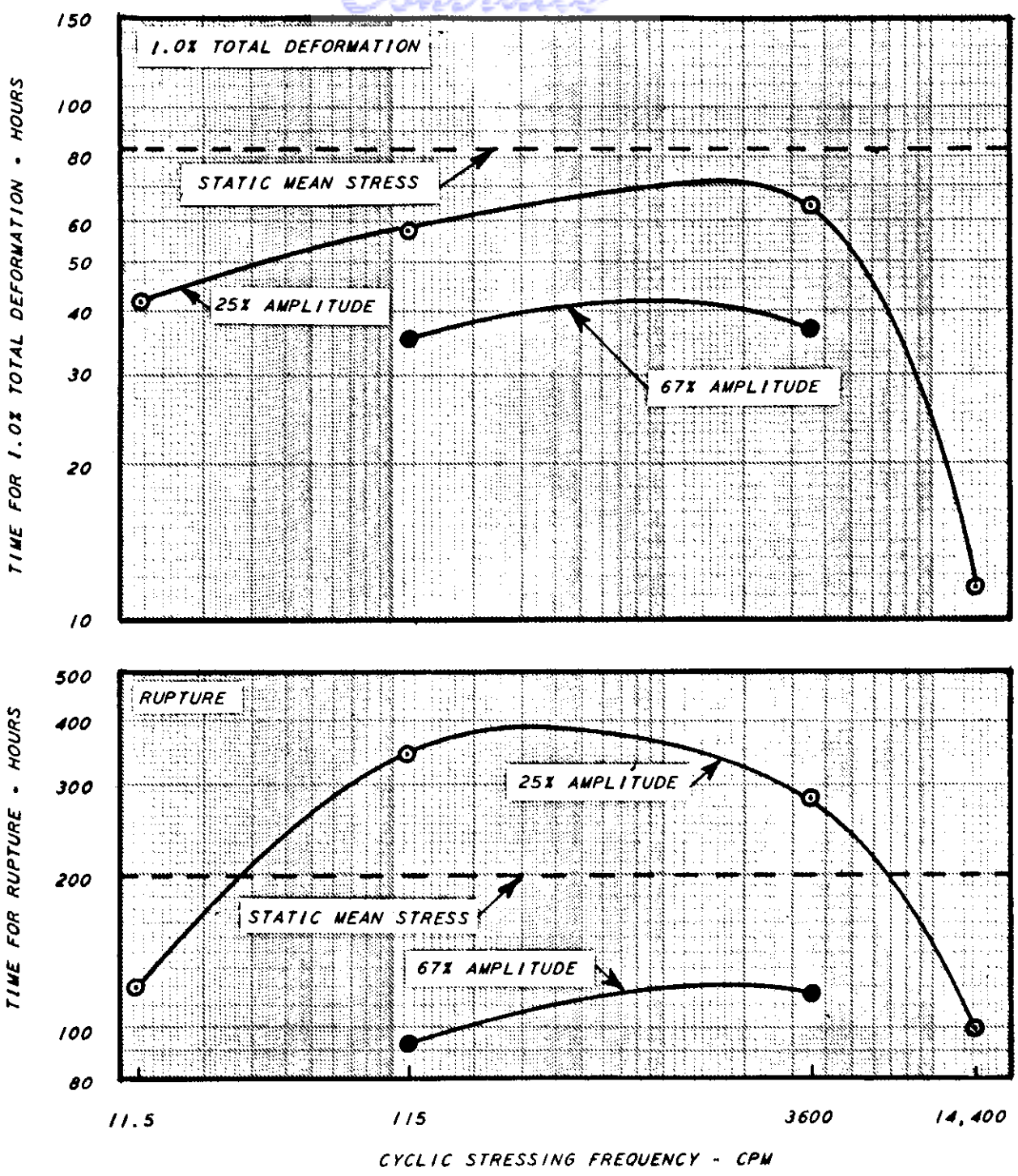

Figure 25 EFFECT OF CYCLIC STRESSING FREQUENCY AND AMPLITUDE ON THE DEFORMATION AND RUPTURE CHARACTERISTICS OF ANNEALED LOW CARBON N-155 SHEET AT 1500°F FOR A CONSTANT MEAN STRESS OF 15,000 PSI

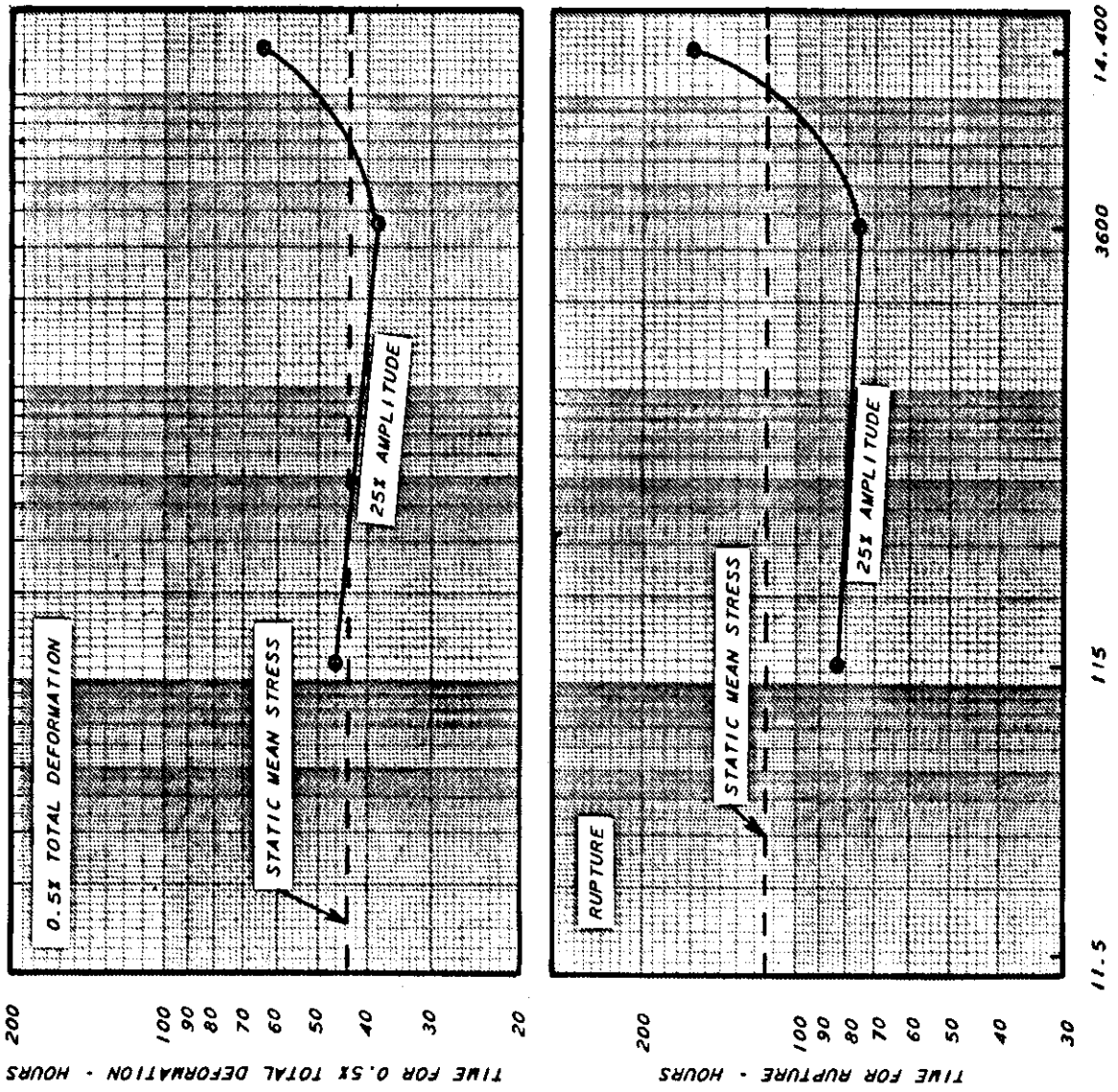

Figure 26 EFFECT OF CYCLIC STRESSING FREQUENCY AND AMPLITUDE ON THE DEFORMATION AND RUPTURE CHARACTERISTICS OF AGED INCONEL X SHEET AT 1350°F FOR A CONSTANT MEAN STRESS OF 35,000 PSI

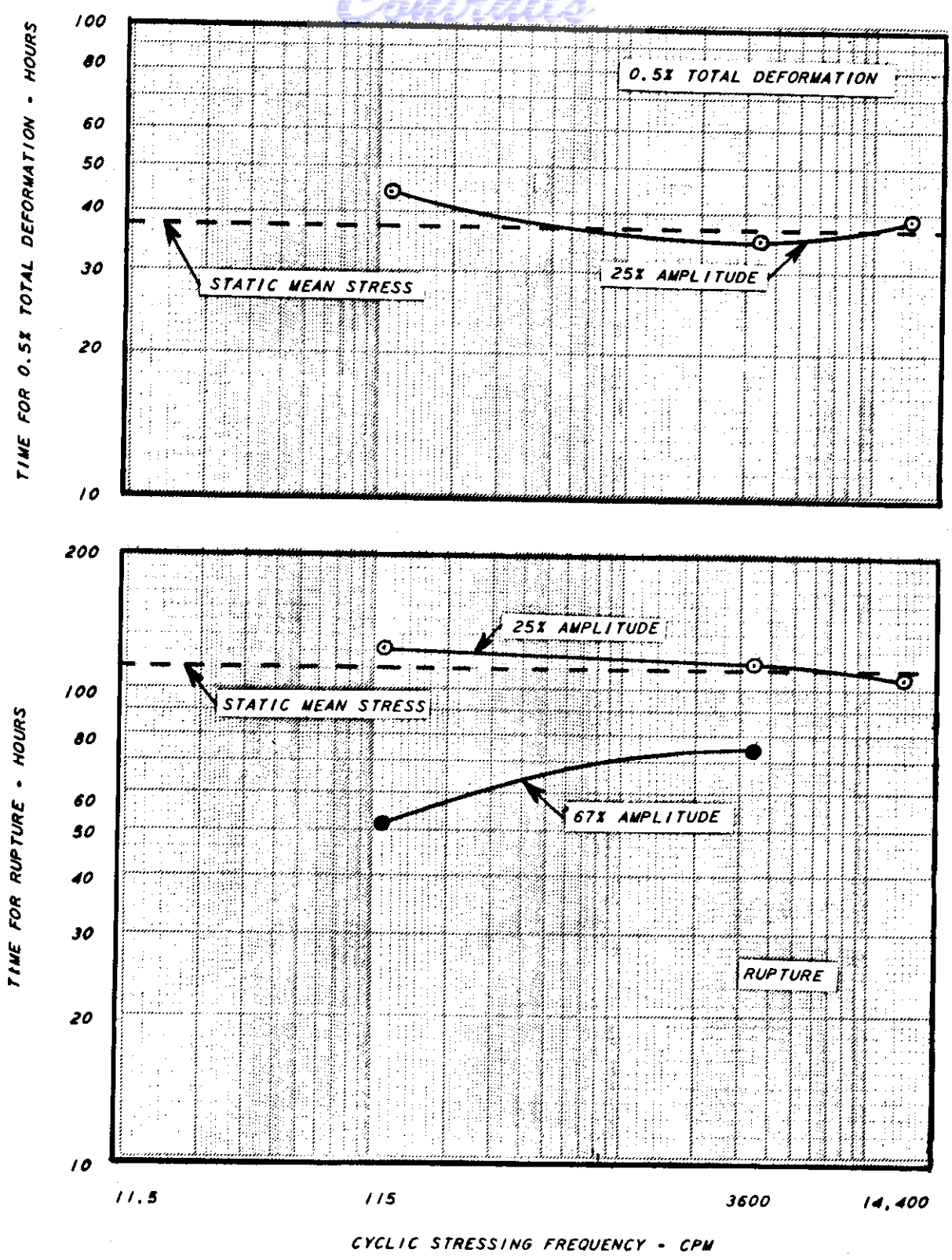

Figure 27 EFFECT OF CYCLIC STRESSING FREQUENCY AND AMPLITUDE ON THE DEFORMATION AND RUPTURE CHARACTERISTICS OF AGED INCONEL X SHEET AT 1500°F FOR A CONSTANT MEAN STRESS OF 16,000 PSI

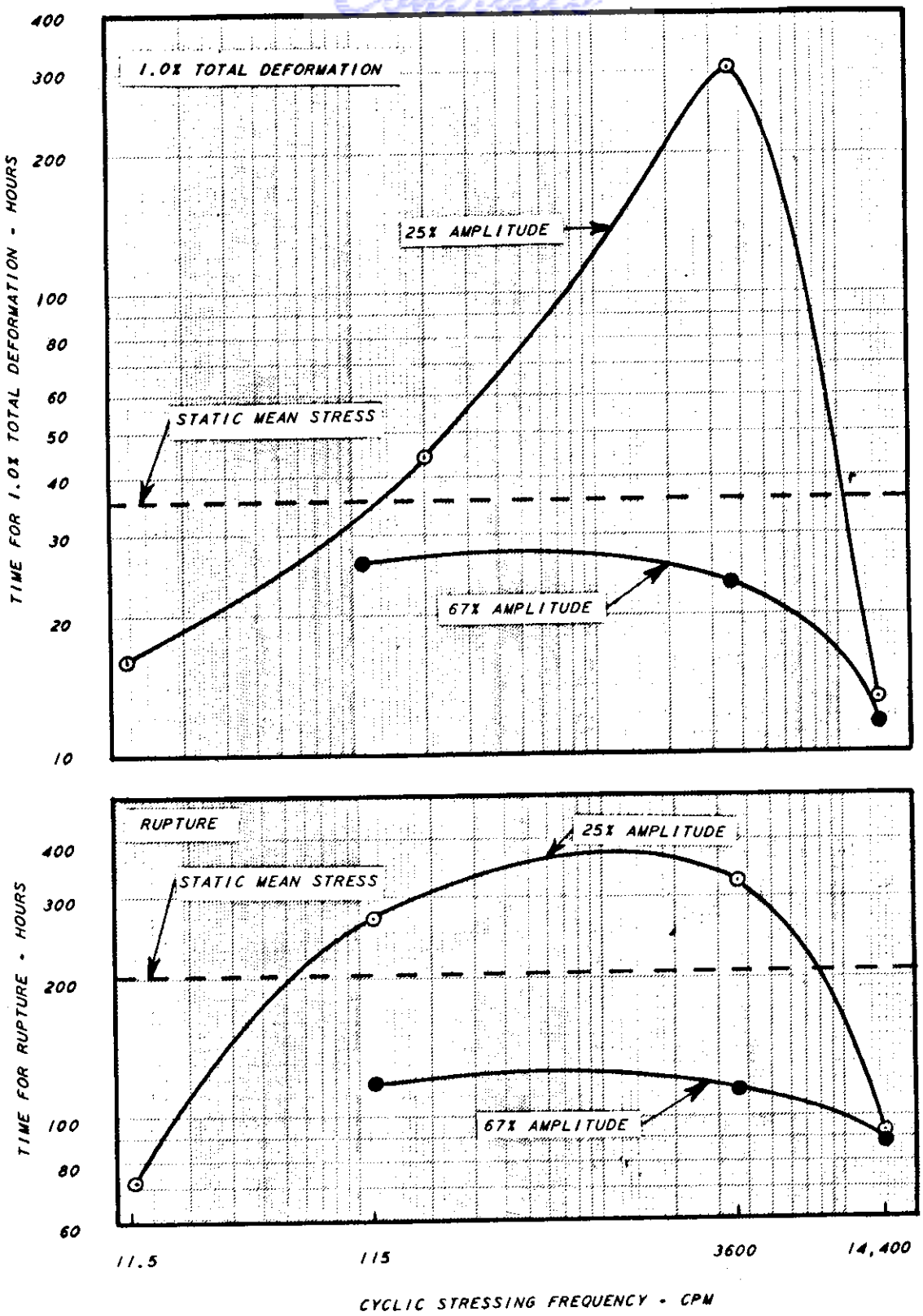

Figure 28 EFFECT OF CYCLIC STRESSING FREQUENCY AND AMPLITUDE ON THE DEFORMATION AND RUPTURE CHARACTERISTICS OF TYPE 321 STAINLESS STEEL SHEET AT 1500°F FOR A CONSTANT MEAN STRESS OF 5000 PSI

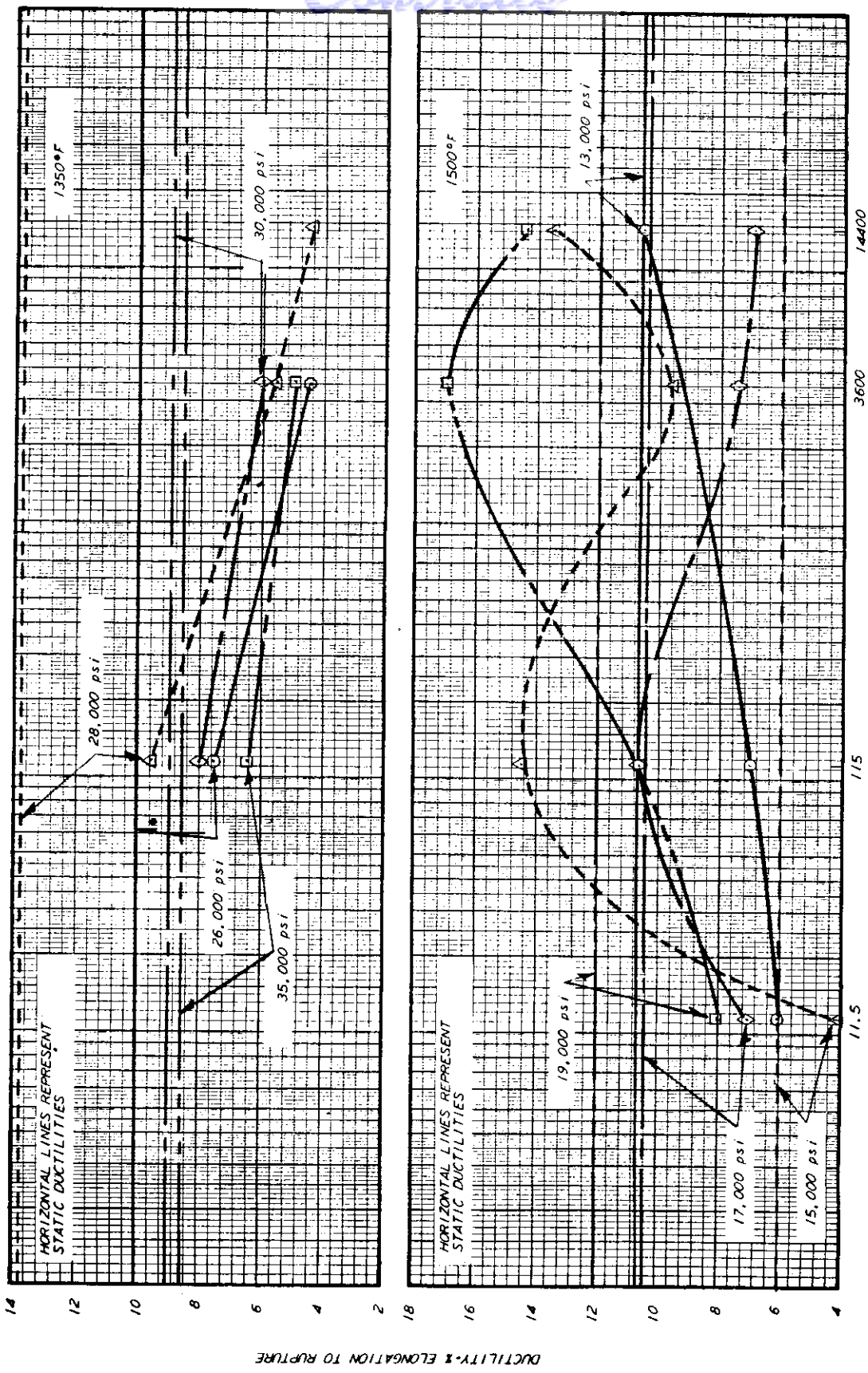

Figure 29 EFFECTS ON RUPTURE DUCTILITY OF ANNEALED LOW CARBON N-155 SHEET RESULTING FROM A ±25% CYCLIC STRESS COMPONENT SUPERIMPOSED UPON STATIC STRESS AT VARIOUS FREQUENCIES

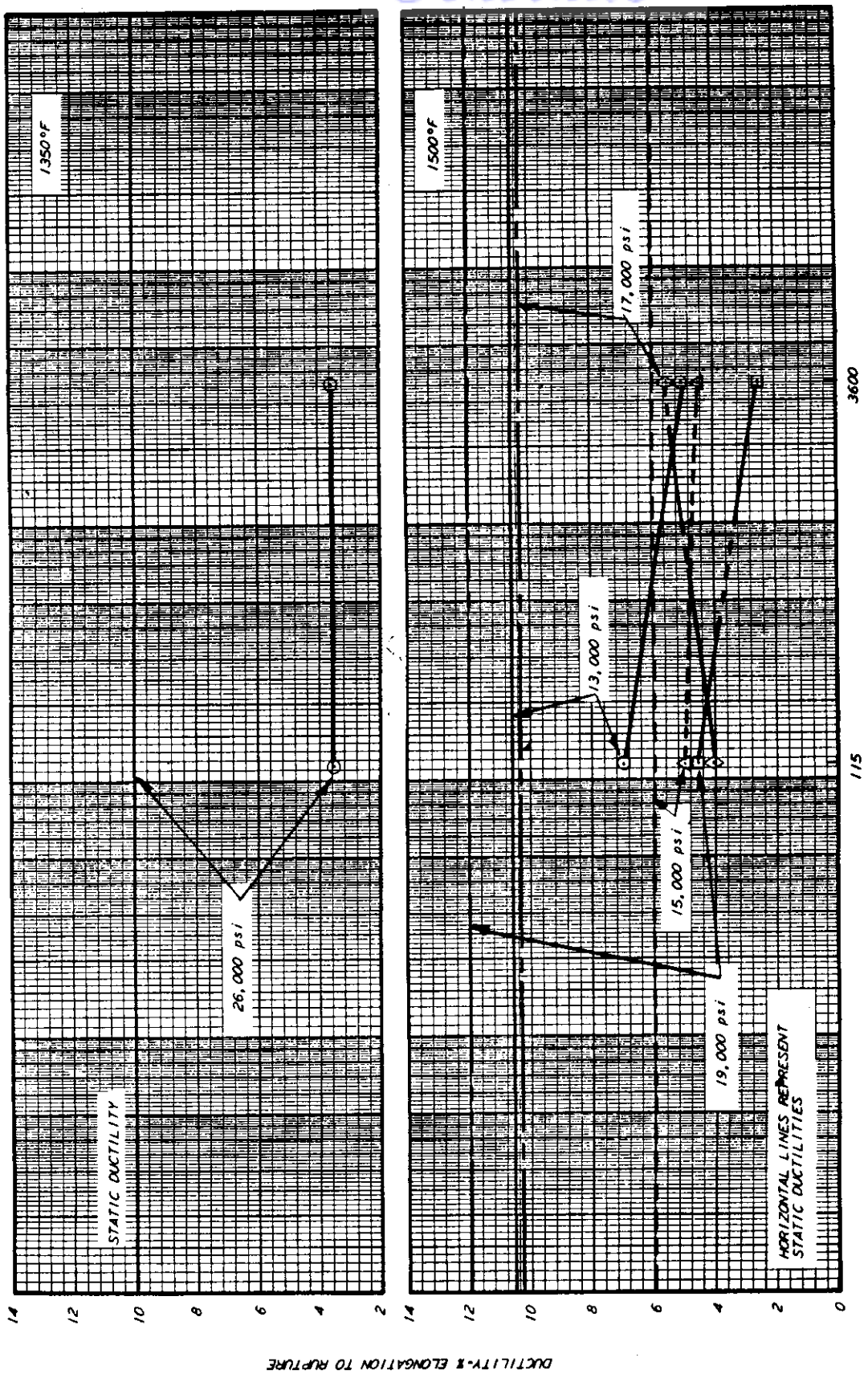

Figure 30 EFFECTS ON RUPTURE DUCTILITY OF ANNEALED LOW CARBON N-155 SHEET RESULTING FROM A ±67% CYCLIC STRESS COMPONENT SUPERIMPOSED UPON STATIC STRESSES AT VARIOUS FREQUENCIES

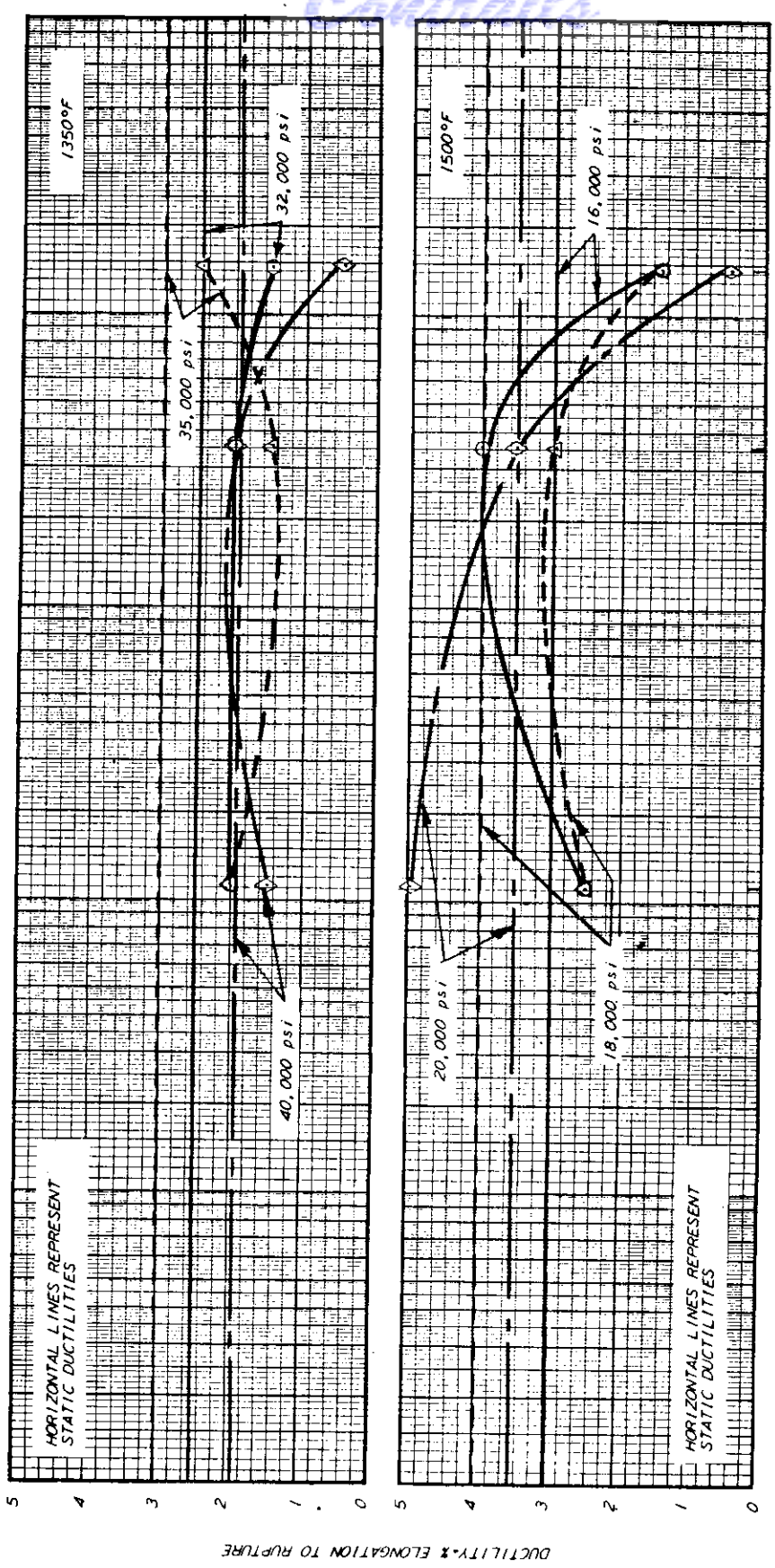

Figure 31 EFFECTS ON RUPTURE DUCTILITY OF AGED INCONEL X SHEET RESULTING FROM A ±25% CYCLIC STRESS COMPONENT SUPERIMPOSED UPON STATIC STRESSES AT VARIOUS FREQUENCIES

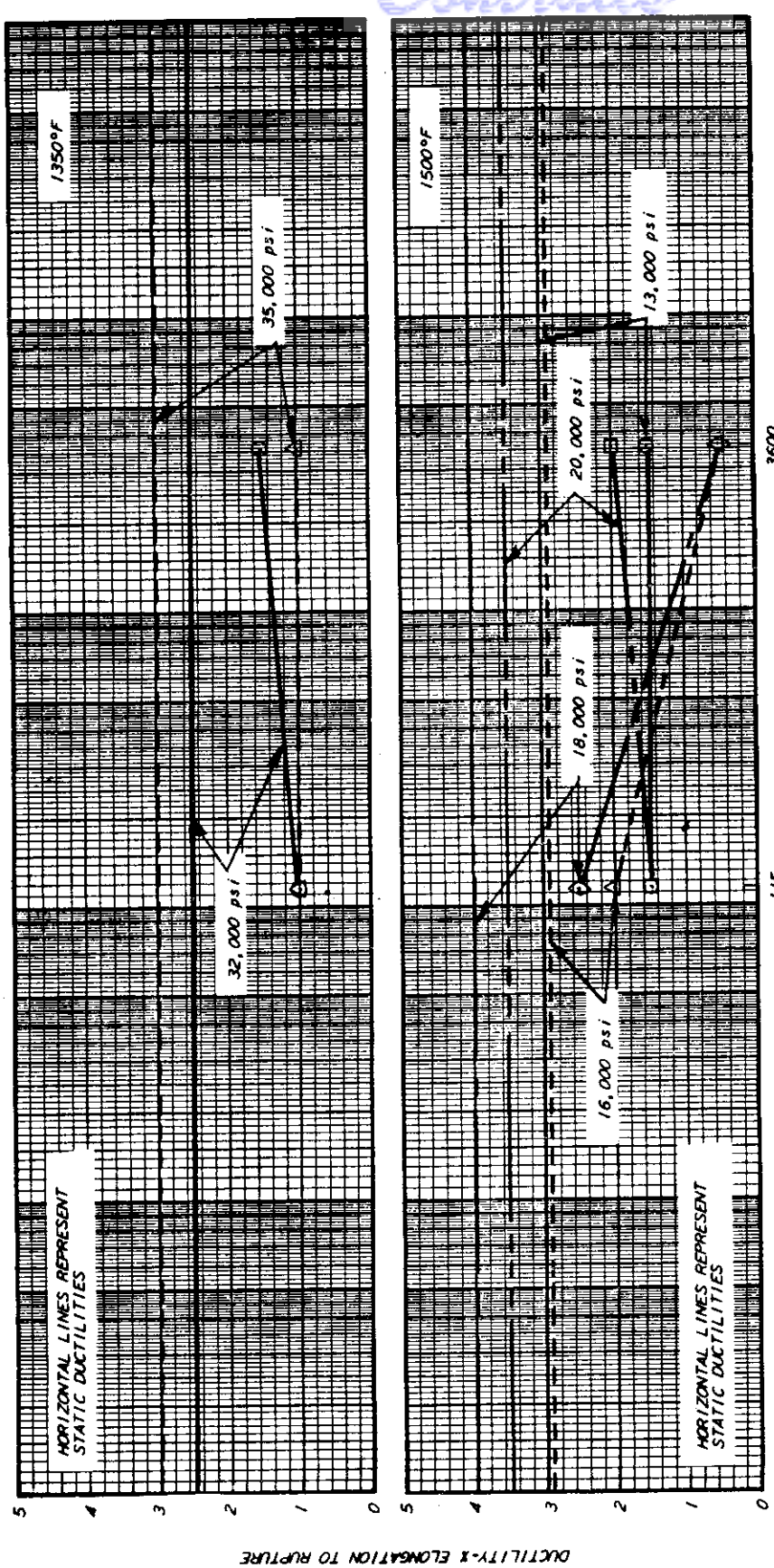

Figure 32 EFFECTS ON RUPTURE DUCTILITY OF AGED INCONEL X SHEET RESULTING FROM A ±67% CYCLIC STRESS COMPONENT SUPERIMPOSED UPON STATIC STRESSES AT VARIOUS FREQUENCIES

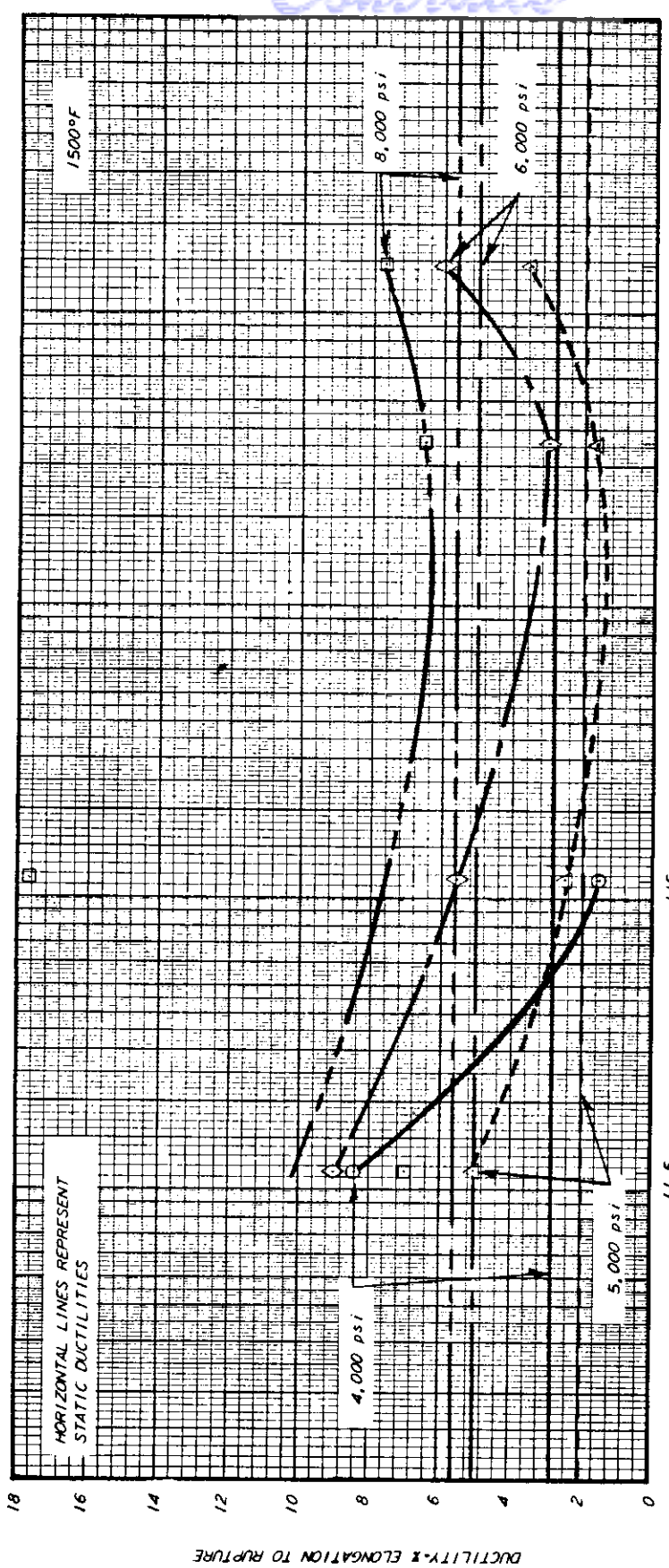

Figure 33 EFFECTS ON RUPTURE DUCTILITY OF TYPE 321 STAINLESS STEEL SHEET RESULTING FROM A ±25% CYCLIC STRESS COMPONENT SUPERIMPOSED UPON STATIC STRESSES AT VARIOUS FREQUENCIES

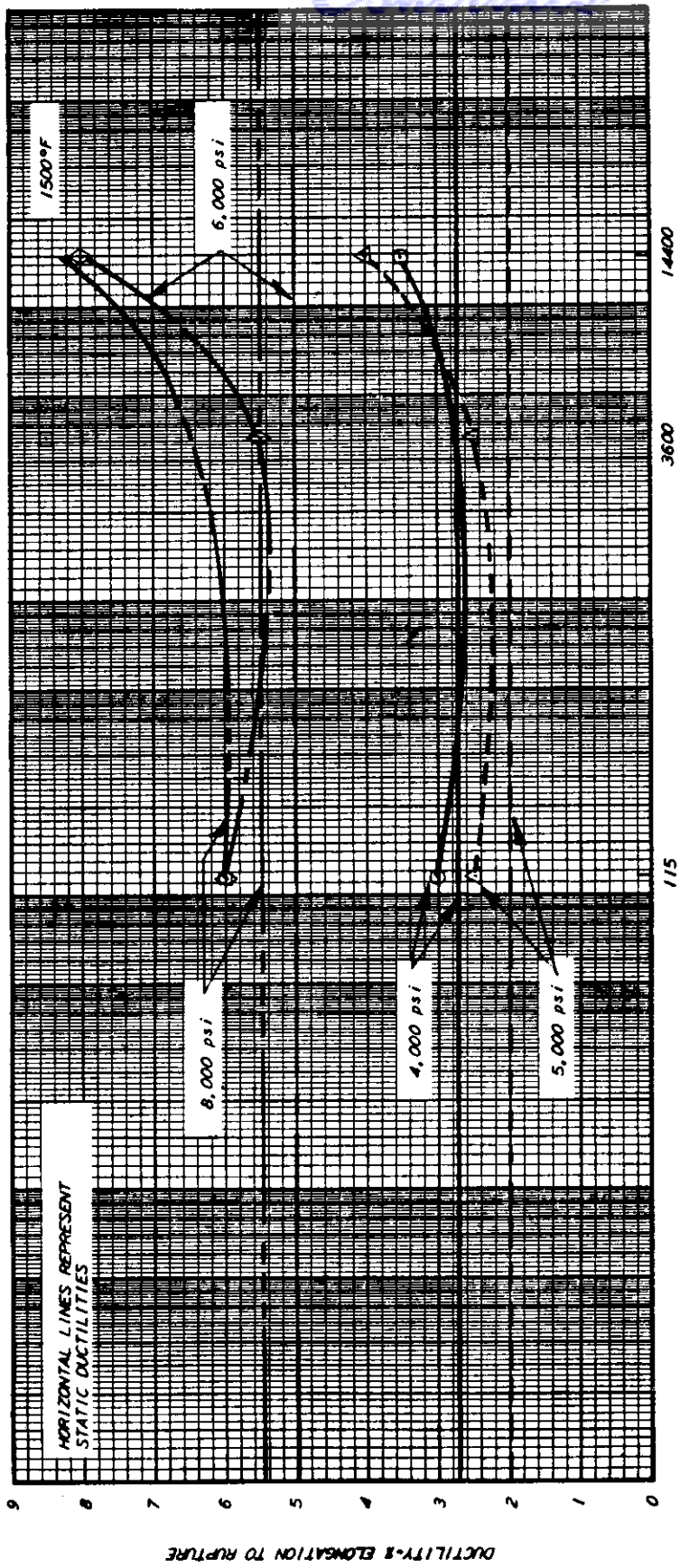

Figure 34 EFFECTS ON RUPTURE DUCTILITY OF TYPE 321 STAINLESS STEEL SHEET RESULTING FROM A ±67% CYCLIC STRESS COMPONENT SUPERIMPOSED UPON STATIC STRESSES AT VARIOUS FREQUENCIES